

We thank the referees for their thoughtful and constructive comments. We have addressed the comments (numbered, below), with referee comments in quotes and italics, and our responses in plain text.

## Referee #1

Major comments:

1. *“Pg 3, line 19: The authors offered clear explanation for the decreasing tendency of SO<sub>2</sub> and NO<sub>x</sub>, which is a result of regulation. However, it seems less clear to me why NH<sub>3</sub> is increasing, although the authors have tied NH<sub>3</sub> emissions with population growth previously. It would be better to explicitly state that the increase of NH<sub>3</sub> emissions is due to the increase of farming activities and fertilizer applications, in order to support the growth of population. I would also suggest adding something about the potential increase of ammonia emission due to global warming, such as the study of Skjøth and Geels 2013. Skjøth, C., and Camilla Geels. "The effect of climate and climate change on ammonia emissions in Europe." Atmospheric Chemistry and Physics 13 (2013): 117-128.”*

To emphasize the relationship between NH<sub>3</sub> emission and population due to food production, we have revised Page 3 Line 11 to “Given that fertilizer usage supports food production for about half the global population (Erisman et al., 2008), NH<sub>3</sub> emissions are linked to world population and so expected to increase into the 21st century (Gerland et al., 2014).” In the introduction, we have added a sentence citing the suggested publication, “Higher temperatures resulting from global warming can also potentially enhance NH<sub>3</sub> emissions (Skjøth and Geels, 2013).”

2. *“Pg 5, line 5. “With high NH<sub>3</sub> concentration, it is somewhat representative of northwestern Europe.” I would suggest the authors to provide additional evidence for this claim. Perhaps, some reference which indicate that northwestern Europe is normally have high NH<sub>3</sub> concentration. Or, maybe provide the averaged NH<sub>3</sub> concentration value on northwestern Europe and compared it with the averaged NH<sub>3</sub> concentration in Cabauw.”*

We have provided more information and noted that Cabauw has high NH<sub>3</sub> levels; “Northwestern Europe has fairly high NH<sub>3</sub> concentrations with yearly averages ranging from 1 to 14 µg m<sup>-3</sup> (median as 4.2 µg m<sup>-3</sup>) for the Netherlands in 2013, reported by the Measuring Ammonia in Nature (MAN) network (Lolkema et al., 2015). Satellite-derived 14 years average for the western Europe is 3 ppbv (~2.3 µg m<sup>-3</sup>) (Warner et al., 2017). Cabauw was somewhat higher due to intensive agriculture in the region with observed yearly NH<sub>3</sub> average of 7.3 ± 6.0 µg m<sup>-3</sup> (~10 ppbv).”

3. *“Pg 6, line 15. “Inorganic ions are also assumed to be only in the aqueous phase.” Does the model assume that all aerosol species are in the aqueous phase or it also consider some of the species in solid state? Please clarify.”*

Yes, we ran the model assuming that all ions are in the aqueous phase. We have revised as “Inorganic ions are also assumed to be only in the aqueous phase (i.e., no solid precipitates).” to minimize confusion.

4. *“Pg 6, line 29. Other studies show that existence of organic phase could also impact the NH<sub>3</sub> and NO<sub>3</sub> partition as some SOA could react with NH<sub>3</sub> and reduce the NH<sub>3</sub> concentration. Add comments. Zhu, S., Horne, J.R., Montoya-Aguilera, J., Hinks, M.L., Nizkorodov, S.A. and Dabdub, D., Modeling reactive ammonia uptake by secondary organic aerosol in CMAQ: application to continental US.”*

We have revised to “This is confirmed by the good agreement between measured and ISORROPIA-II predicted NH<sub>3</sub>-NH<sub>4</sub><sup>+</sup> partitioning without considering organic acids or other organic species (see section 3.2). Although recent modeling study has suggested that ambient NH<sub>3</sub> concentration can be decreased by as much as 31% in winter and 67% in summer in the US, due to the reactive uptake of NH<sub>3</sub> by secondary carbonyl compounds (Zhu et al., 2018), this process doesn’t appear to have an impact on NH<sub>3</sub>-NH<sub>4</sub><sup>+</sup> partitioning and predicted pH for the locations in this study.”

With the above said, it is also important to note that even if NH<sub>3(g)</sub> were reduced by 30-60% by reactions with the organic phase, the impact on aerosol acidity would be modest (change of about 0.1-0.2 pH units) given that an order of magnitude change in ambient NH<sub>3</sub> concentration is required for pH levels to be changed by one unit (Guo et al., 2017b).

5. *“Pg 7, line 4-5. The authors used two “discussed below” in this sentence. It would be better to give the exact section or location of the discussion instead. Does it refer to the first paragraph of 2.3? Actually, there is research showing that different mixing assumption could have significant impact on NO<sub>3</sub>- and NH<sub>4</sub><sup>+</sup> partition, especially on NO<sub>3</sub>-: Zhu, S., Sartelet, K., Zhang, Y. and Nenes, A., 2016. Three-dimensional modeling of the mixing state of particles over Greater Paris. Journal of Geophysical Research: Atmospheres, 121(10), pp.5930-5947.”*

We have provided the sections that we refer to, “(discussed below in Section 2.3)...(discussed below in Section 3.2 and also see Table S1)”. Thanks for pointing out this paper, we have cited it in the manuscript. We have not discussed it in detail since it follows the less quantitative approach of assuming nitrate only forms once sulfate is fully neutralized (i.e., NH<sub>4</sub><sup>+</sup>/SO<sub>4</sub><sup>2-</sup> ratios above 2), instead of a rigorous thermodynamic analysis, the focus of this paper.

6. *“P11, line 15. The authors should provide more details regarding to the nature of “particle artifacts in the gas collection system” that is affecting the measurement of HNO<sub>3</sub> and HCl.”*

We have edited this, removing speculation on the cause. It now reads, “However, for unknown reasons, gas-phase components of these two species showed significant discrepancies (R<sup>2</sup> of 0.13 to 0.17). We note that it may be associated with the very low gas phase concentrations of these species, in contrast to NH<sub>3</sub>.”

7. *“Pg 17, line 19. Since the calculations are based on site measurement in this study, does it suggest that the pH calculated here is closer to the reality than the one calculated by Pozzer et al., (2017). Or, on the other hand, is it possible that the measurements site is not representative enough for the larger domain used in the global model calculation due to its coarse resolution? Are there any regional simulation results that is consistent with the pH prediction presented here?”*

This is a good point. Pozzer et al. (2017) did not publish any  $\text{NH}_3$  concentration, which could be used for comparison with observations in Cabauw. Other relevant regional simulated pH could also not be found for the same region. Pozzer et al. (2017) published an average pH for Europe of  $\sim 2$ , which is 1.7 units lower than the one-year pH in Cabauw. This may indicate that the Cabauw sampling site is not representative of Europe in general (the Pozzer's paper), but a detailed comparison between the two model inputs is necessary to understand the cause of the pH difference. As noted above (and in the revised manuscript), the Cabauw site has higher  $\text{NH}_3$  concentrations, which will increase particle pH. Holding all other model inputs constant, a factor of 10 lower  $\text{NH}_3$  decreases pH by roughly one unit (as shown in Figure 3). Based on satellite derived 14-year  $\text{NH}_3$  average (3 ppb and  $2.3 \mu\text{g m}^{-3}$ ) for western Europe as an example (Warner et al., 2017), the pH in Cabauw decrease to around 3 for the one-year average and winter average, and below 3 for summer, according to the linear fitting lines in Figure 3. Meteorological conditions and particle composition also contribute to the difference in pH prediction mentioned above. Although it has been found that inaccurate treatment of nonvolatile cations may cause overestimation of particle pH in regional models (Vasilakos et al., 2018), it doesn't explain the above pH difference since the modeled pH in Pozzer et al. (2017) (from global modeling) is the lower one and the levels of nonvolatile cations are low in Cabauw. Despite of the difference in pH, we believe the findings of Pozzer et al, (2017) are consistent with the framework established in this study, that is a critical pH of  $\sim 3$ . Since the Pozzer's European pH is 2, below 3, controlling  $\text{NH}_3$  emission is suggested as an effective way to reduce particle mass.

8. *“Pg 18, line 13-14. This conclusion looks not very convincing to me. Since the particle composition is so different between SE US and NE US, the author should justify how the SE US could be a representative case for the eastern US in the summer, and how the NE US could be representative case for the eastern US in the winter before drawing such a conclusion. Or latest explain the cause of such a high sulfate composition (76%) in the SE US case.”*

We have clarified the statement as suggested by the reviewer. The SE US simulation is only representative of the SE US; the same for the NE US simulation. Now the text becomes “Therefore, it is more effective to control  $\text{NH}_x$  in winter in the NE US and  $\text{SO}_4^{2-}$  in summer in SE US, a finding consistent with previous studies (Duyzer, 1994; Tsimpidi et al., 2007).” The large fraction of sulfate is a result of the small fraction of nitrate. In such situations, ammonium basically tracks sulfate. Due to the difference in molecular weight, sulfate is the dominant inorganic mass. We have added a sentence explaining the reason, “A small fraction of nitrate aerosol is typically observed in the southeast in summer (Hidy et al., 2014) due to the high temperature and low particle pH.”

Minor comments:

9. “Pg 5, line 13, the word “alternatively” here is confusing. Do you mean it is the first hour measurement is for PM<sub>1</sub> and the next hour will be for PM<sub>2.5</sub>? In that case the measurement interval will be 2 hours for either PM<sub>1</sub> or PM<sub>2.5</sub>, is that the case? Please clarify.”

A clarification is made. “...alternatively between PM<sub>1</sub> and PM<sub>2.5</sub>, each size sampled hourly (i.e., a two-hour interval for one size; a one-hour interval for gas).”

10. “Pg 7, line 9. “In Cabauw, it has been reported...” Could reference be provided for this report?”

The reference “(Schlag et al., 2017)” was there in the middle of the sentence. Since it is not obvious, we have moved it to the end.

11. “Pg 7, line 25. It would be better to specify the “coarse mode salts” that HNO<sub>3</sub> evolved into.”

We have added examples as “coarse mode salts (e.g., NaCl and CaCl<sub>2</sub>)”.

12. “Pg 9, line 14. “0.987x10<sup>-14</sup> is a unit conversion factor” I would better to specify which units are being converted with this factor.”

We have added explanation as “where  $0.987 \times 10^{-14}$  is a unit conversion factor (from converting atm and  $\mu\text{g}$  to SI units)”.

13. “Pg 10, line 3. Could the authors be more specific on how the “approximately 0.6” nonideality shifts are calculated? Or provide a reference S curve without the non-ideality effect?”

The 0.6 unit pH difference is provided by comparing nitrate partitioning S curves calculated assuming  $\gamma_{\text{NO}_3^-} \gamma_{\text{H}^+} = 1$  (ideal) and 0.24 (non-ideal; from ISORROPIA). More specifically, compare pH<sub>50</sub> values for the two S curves. A figure is provided to visualize the difference and added to supplemental material as the new Fig. S2.

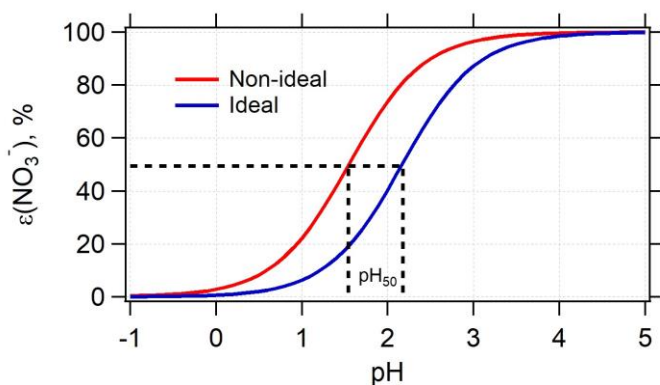




Figure. Predicted particle phase fraction of total nitrate,  $\varepsilon(\text{NO}_3^-)$ , versus pH for one-year average condition in Cabauw based on Eq. (4). The red and blue lines are based on  $\gamma_{\text{NO}_3^-}\gamma_{\text{H}^+} = 0.24$  and 1, respectively.

14. *“P11, line 17. Could the authors provide the references for those “previous studies” mentioned here?”*

A reference has been added.

15. *“P12, line 2. Could the authors provide the exact hour ranges used in this study to define “night” and “daytime”?”*

We define “night” and “day” by sunrise and sunset. However, we don’t have solar radiation data to plot a diurnal profile. Since sunrise and sunset time can vary substantially from summer to winter, we cannot provide exact hour ranges. For example, daytime is from 05:24 to 22:03 on June 1 2013 and from 08:48 to 16:38 on Dec 31 2013. To minimize confusion, we have revised the text to exact hours which are not as affected by seasonal changes in sunrise and sunset, “A diurnal pattern of ambient particle pH is observed in Cabauw, similar to other studies (Guo et al., 2015). For example, for the nighttime period of 1 am to 7 am, the average pH is 3.9, whereas for the daytime period of 1 pm to 6 pm the pH is 3.5. The difference is mainly driven by the diurnal variation in liquid water content (see Fig. S1)”.

16. *“Pg 12, line 13. I found it confusing that the authors keep changing between “NE US” and “WINTER” for the Guo et al., (2016) case, for example, “WINTER” is used in Figure 2, but “NE US” is used here in the text. I suggest the authors use more consistent expression.”*

We have revised the Figure 2 legends to separate the SOAS and WINTER studies. The SOAS study is under the “Southeastern US” and the WINTER study is under the “Northeastern US”. Hopefully, this clarifies the issue.

17. *“Pg 19, line 4. The previous discussions in this paragraph are based on Cabauw winter and Beijing, while the 19%“(NH<sub>4</sub><sup>+</sup>) value used here are from one-year Cabauw, would you explain why?”*

Thanks for pointing it out! We have replaced “19%” with “27%”, which was the right number for Cabauw winter average.

18. *“Pg 20, line 12. What does “further from the actual ambient particle pH” referred for? Do you mean the region 2 of the curve is further from the ambient particle pH?”*

Yes, we mean region 2 or pH<sub>50</sub>. We have revised to “This is explained by a shift in the HNO<sub>3</sub>-NO<sub>3</sub><sup>-</sup> partitioning ( $\varepsilon(\text{NO}_3^-)$ ) curve to lower pH in winter and pH<sub>50</sub> (where  $\varepsilon(\text{NO}_3^-) = 50\%$ ) further from the actual ambient particle pH.”.

## Referee #2

Major comments:

1. *“The authors introduce a new conceptual framework to explain seasonal and regional differences in the sensitivity of particulate matter to ammonia emissions. This has potential policy implications and it would be useful for the authors to compare with other techniques that have been used previously to highlight potential differences.*

*In particular, previous studies have used the gas-ratio from Ansari and Pandis to interpret global model results (see for instance Pinder et al. (2007, 2008), Paulot (2016), Pozzer et al., 2017)  $GR = (TNH_4 - 2 \cdot TSO_4)/TNO_3$  with  $0 < GR < 1$  indicating sensitivity to  $NH_x$  and  $GR > 1$  indicating sensitivity to  $NH_3$ .*

*Obviously, this cannot directly address variations associated with seasonality. However, based on the information provided in Table S1,  $GR < 1$  only for SE US, Virginia, and Pasadena. In other words the weak sensitivity of nitrate to ammonia emissions at the other sites could be inferred simply from concentrations, which is consistent with the findings of the studies mentioned earlier.*

*In addition, many global models do not use ISORROPIA but simpler (cheaper) aerosol thermodynamic models (see for instance Bellouin et al (2011), Hauglustaine (2014)). Such schemes, which do not explicitly account for aerosol pH, will also simulate a nonlinear response of ammonium nitrate to changes in ammonia emissions (see equation A8 in Bellouin et al (2011)). It would be useful for the authors to show how different the response of nitrate and ammonium to changes in ammonia/ $NO_x$  emissions (i.e., Fig 5) would be using such approach.*

*In particular, this would help strength the case for thinking in terms of aerosol pH rather than simply in terms of concentrations.”*

The reviewer raises an important and very broad question. First we note that global models use aerosol thermodynamic modules of all levels of complexity (some not at all). All these models would predict some degree of nonlinearity because one of the precursors,  $NH_3$  or  $HNO_3$ , become limiting. Our point is that using pH to look at the sensitivity of nitrate to the precursors is new. It makes things simpler and provides a more fundamental understanding of the processes involved. Furthermore, even if the models have the correct thermodynamics they can still get the sensitivity wrong due to a biased predicted pH, as we note with the reference to Vasilakos et al. (2018). We feel that the degree to which each implementation differs, and how it compares with the usage of pH as a control parameter requires a dedicated publication in itself.

We have added some text to try and clarify these points. The next now reads:

“Large-scale models to assess effectiveness of  $NH_3$  control requires good predictions of a range of pertinent emissions and sinks ( $NH_3$ ,  $NO_x$ ,  $SO_2$ , and nonvolatile cations), and accurate representation of their applicable atmospheric chemical processes. Thermodynamic modules

of different levels of complexity are then applied to determine sensitivities to the precursors (e.g.,  $\text{NH}_3$ ,  $\text{HNO}_3$ ). In some cases (Pozzer et al., 2017), the aerosol pH is explicitly determined with an embedded thermodynamic model, such as ISORROPIA-II (Fountoukis and Nenes, 2007). Due to the complexities from all these factors, chemical transport model-predicted responses to changing emissions may not align with observations. For example, the sensitivity of  $\text{PM}_{2.5}$  pH in the Community Multiscale Air Quality (CMAQ) simulations to the mass of crustal material apportioned to the  $\text{PM}_{2.5}$  size range can have important effects on anticipated responses to these changing emission trends. Vasilakos et al. (2018) have shown that including too much crustal material in  $\text{PM}_{2.5}$  results in a predicted increasing trend in both aerosol pH and concentrations of  $\text{NH}_4\text{NO}_3$ , which is counter to observations (Weber et al., 2016).

Overall, calculating aerosol pH is a more accurate approach that provides a fundamental understanding of the factors controlling  $\text{HNO}_3$ - $\text{NO}_3^-$  partitioning and therefore enables a direct evaluation of different studies. Furthermore, it is also useful to determine aerosol pH since it has broad application to many other important aerosol processes. For instance, pH is a mediator of many heterogeneous chemical processes, including various acid-catalyzed reactions (Jang et al., 2002; Eddingsaas et al., 2010; Surratt et al., 2010), gas-particle partitioning of species other than  $\text{HNO}_3$  and  $\text{NH}_3$ , such as organic acids and halogens (Fridlind and Jacobson, 2000; Young et al., 2013; Guo et al., 2017a; Nah et al., 2018), and solubility of metals and other nutrient species (Meskhidze et al., 2003; Nenes et al., 2011; Longo et al., 2016; Stockdale et al., 2016; Fang et al., 2017).

In this study, we apply a more direct approach, where measured gas and particle concentrations and the thermodynamic model ISORROPIA-II are used directly in a sensitivity analysis to evaluate the effectiveness of  $\text{NH}_3$  emission controls on fine particle mass relative to  $\text{NO}_x$  control. Contrasts are made between sites that have a wide range in  $\text{NH}_3$  concentrations and aerosol composition, ...”

2. *“I am not convinced by the current discussion of the impact of  $\text{NH}_3$  emissions controls on nitrogen deposition. The authors argue that lowering aerosol pH (via lower  $\text{NH}_3$  emissions) will modify the ratio of reduced to oxidized nitrogen deposition. However, it is unclear why this is important (no reference is given), especially considering the benefits of lower  $\text{NH}_x$  deposition and the existence of other removal pathways (wet deposition) that may not exhibit the same sensitivity to the  $\text{NH}_4/\text{NH}_3$  partitioning. A longer discussion is needed given that this conclusion is highlighted in the abstract.”*

We were only focusing here on effects on dry deposition since the paper discusses relative gas and particle concentrations and we note the large differences in gas/particle deposition velocities. Discussing effects of N deposition due to wet processing is beyond the scope of this paper. However, the reviewer's point that it may be more complicated is well taken. We have modified the text to be more precise and note complicating effects of wet removal processes.

In the abstract, it has been revised to “Finally, controlling  $\text{NH}_3$  emissions to increase aerosol acidity and evaporate  $\text{NH}_4\text{NO}_3$  will have other effects, beyond reduction of  $\text{PM}_{2.5}$   $\text{NH}_4\text{NO}_3$ , such as increasing aerosol toxicity and potentially altering the deposition patterns of nitrogen and trace nutrients.”

In the section 3.5, “Lowering particle pH through  $\text{NH}_3$  reductions will decrease overall reduced nitrogen deposition but may results in more localized oxidized nitrogen dry deposition if the lower pH results in  $\text{NO}_3^-$  evaporation and higher  $\text{HNO}_3$  concentrations. Deposition due to wet removal processes are not considered here.”

3. *“the authors focus on seasonal averages. It would be interesting to discuss whether the sensitivity of particulate matter to  $\text{NH}_3$  emissions is different depending on the concentration of  $\text{NO}_3^-$  and whether this would affect the probability distribution of PM under the different emission reduction scenarios shown in Fig. 5. This may be important for policy makers as some standards are based on 24hr averages ([https://www3.epa.gov/ttn/naaqs/standards/pm/s\\_pm\\_history.html](https://www3.epa.gov/ttn/naaqs/standards/pm/s_pm_history.html))”*

We understand the point raised. The main issue with this suggestion is that the sensitivity of particulate matter to  $\text{NH}_3$  (or  $\text{HNO}_3$ ) emissions is directly determined by the aerosol pH. Otherwise, the sensitivity can take a wide range of values for constant  $\text{NO}_3^-$ , as the pH can still vary considerably. We believe that this shift in approach (first looking at pH and then seeing how that affects aerosol sensitivity to emissions), is one of the most important messages of the paper. Towards that, a simpler approach, the  $\text{HNO}_3$ - $\text{NO}_3^-$  S curve (in Section 2.3), is provided to roughly estimate the effectiveness of  $\text{NH}_3$  control.

Technical comments:

4. *“p4 line 5  $\text{NH}_3$  can also enhance the in-cloud oxidation of  $\text{SO}_2$  by  $\text{O}_3$ . See for instance Wang (2011) or Paulot (2017)”*

Thanks for bringing attention to these references. We have revised the text to “Reduction in  $\text{NH}_3$  also reduces the amount of  $\text{NH}_4^+$  associated with sulfates and lowers the pH-dependent sulfate production rate, such as in cloud  $\text{SO}_2$  oxidation by  $\text{O}_3$  (Wang et al., 2011; Cheng et al., 2016; Paulot et al., 2017), and the interplay between the two species may drive much of the sensitivity of  $\text{PM}_{2.5}$  to  $\text{NH}_3$  and  $\text{NO}_x$  reductions (e.g., (Vasilakos et al., 2018))”.

5. *“p17 line 15 I believe livestock emissions are likely to dominate ammonia emissions in summer.”*

We had thought that as well, but literature studies do not seem to agree. Based on Figure 7 in Zhang et al. (2018), livestock waste dominates in winter rather than summer. The annual emissions from fertilizer and livestock waste are quite similar (5.05 vs 5.31  $\text{Tg a}^{-1}$ ).

6. *“dash black line Fig. 4 not defined”*

We apologize for this oversight. The black dash lines in the pH figures identifies the critical pH value of 3, and now has been noted in the caption.

## References

- Cheng, Y., Zheng, G., Wei, C., Mu, Q., Zheng, B., Wang, Z., Gao, M., Zhang, Q., He, K., Carmichael, G., Poschl, U., and Su, H.: Reactive nitrogen chemistry in aerosol water as a source of sulfate during haze events in China, *Sci. Adv.*, 2, e1601530, doi: 10.1126/sciadv.1601530, 2016.
- Duyzer, J.: Dry deposition of ammonia and ammonium aerosols over heathland, *J. Geophys. Res.*, 99, 18757-18763, doi: 10.1029/94jd01210, 1994.
- Eddingsaas, N. C., VanderVelde, D. G., and Wennberg, P. O.: Kinetics and Products of the Acid-Catalyzed Ring-Opening of Atmospherically Relevant Butyl Epoxy Alcohols, *J. Phys. Chem. A*, 114, 8106-8113, doi: 10.1021/Jp103907c, 2010.
- Fang, T., Guo, H., Zeng, L., Verma, V., Nenes, A., and Weber, R. J.: Highly Acidic Ambient Particles, Soluble Metals, and Oxidative Potential: A Link between Sulfate and Aerosol Toxicity, *Environ. Sci. Technol.*, 51, 2611-2620, doi: 10.1021/acs.est.6b06151, 2017.
- Fountoukis, C., and Nenes, A.: ISORROPIA II: a computationally efficient thermodynamic equilibrium model for  $K^+$ - $Ca^{2+}$ - $Mg^{2+}$ - $NH_4^+$ - $Na^+$ - $SO_4^{2-}$ - $NO_3^-$ - $Cl^-$ - $H_2O$  aerosols, *Atmos. Chem. Phys.*, 7, 4639-4659, doi: 10.5194/acp-7-4639-2007, 2007.
- Fridlind, A. M., and Jacobson, M. Z.: A study of gas-aerosol equilibrium and aerosol pH in the remote marine boundary layer during the First Aerosol Characterization Experiment (ACE 1), *J. Geophys. Res.*, 105, 17325-17340, doi: 10.1029/2000jd900209, 2000.
- Guo, H., Xu, L., Bougiatioti, A., Cerully, K. M., Capps, S. L., Hite, J. R., Carlton, A. G., Lee, S. H., Bergin, M. H., Ng, N. L., Nenes, A., and Weber, R. J.: Fine-particle water and pH in the southeastern United States, *Atmos. Chem. Phys.*, 15, 5211-5228, doi: 10.5194/acp-15-5211-2015, 2015.
- Guo, H., Liu, J., Froyd, K. D., Roberts, J. M., Veres, P. R., Hayes, P. L., Jimenez, J. L., Nenes, A., and Weber, R. J.: Fine particle pH and gas-particle phase partitioning of inorganic species in Pasadena, California, during the 2010 CalNex campaign, *Atmos. Chem. Phys.*, 17, 5703-5719, doi: 10.5194/acp-17-5703-2017, 2017a.
- Guo, H., Weber, R. J., and Nenes, A.: High levels of ammonia do not raise fine particle pH sufficiently to yield nitrogen oxide-dominated sulfate production, *Sci. Rep.*, 7, doi: 10.1038/s41598-017-11704-0, 2017b.
- Hidy, G. M., Blanchard, C. L., Baumann, K., Edgerton, E., Tanenbaum, S., Shaw, S., Knipping, E., Tombach, I., Jansen, J., and Walters, J.: Chemical climatology of the southeastern United States, 1999-2013, *Atmos. Chem. Phys.*, 14, 11893-11914, doi: 10.5194/acp-14-11893-2014, 2014.
- Jang, M., Czoschke, N. M., Lee, S., and Kamens, R. M.: Heterogeneous atmospheric aerosol production by acid-catalyzed particle-phase reactions, *Science*, 298, 814-817, doi: 10.1126/science.1075798, 2002.
- Lolkema, D. E., Noordijk, H., Stolk, A. P., Hoogerbrugge, R., van Zanten, M. C., and van Pul, W. A. J.: The Measuring Ammonia in Nature (MAN) network in the Netherlands, *Biogeosciences*, 12, 5133-5142, doi: 10.5194/bg-12-5133-2015, 2015.
- Longo, A. F., Feng, Y., Lai, B., Landing, W. M., Shelley, R. U., Nenes, A., Mihalopoulos, N., Violaki, K., and Ingall, E. D.: Influence of Atmospheric Processes on the Solubility and Composition of Iron in Saharan Dust, *Environ Sci Technol*, 50, 6912-6920, doi: 10.1021/acs.est.6b02605, 2016.
- Meskhidze, N., Chameides, W. L., Nenes, A., and Chen, G.: Iron mobilization in mineral dust: Can anthropogenic  $SO_2$  emissions affect ocean productivity?, *Geophys. Res. Lett.*, 30, 2085, doi: 10.1029/2003gl018035, 2003.
- Nah, T., Guo, H., Sullivan, A. P., Chen, Y., Tanner, D. J., Nenes, A., Russell, A., Ng, N. L., Huey, L. G., and Weber, R. J.: Characterization of Aerosol Composition, Aerosol Acidity and Organic Acid Partitioning at an Agriculture-Intensive Rural Southeastern U.S. Site, *Atmos. Chem. Phys. Disc.*, 1-46, doi: 10.5194/acp-2018-373, 2018.

- Nenes, A., Krom, M. D., Mihalopoulos, N., Van Cappellen, P., Shi, Z., Bougiatioti, A., Zarmas, P., and Herut, B.: Atmospheric acidification of mineral aerosols: a source of bioavailable phosphorus for the oceans, *Atmos. Chem. Phys.*, 11, 6265-6272, doi: 10.5194/acp-11-6265-2011, 2011.
- Paulot, F., Fan, S., and Horowitz, L. W.: Contrasting seasonal responses of sulfate aerosols to declining SO<sub>2</sub> emissions in the Eastern U.S.: Implications for the efficacy of SO<sub>2</sub> emission controls, *Geophys. Res. Lett.*, 44, 455-464, doi: 10.1002/2016gl070695, 2017.
- Pozzer, A., Tsimpidi, A. P., Karydis, V. A., de Meij, A., and Lelieveld, J.: Impact of agricultural emission reductions on fine-particulate matter and public health, *Atmos. Chem. Phys.*, 17, 12813-12826, doi: 10.5194/acp-17-12813-2017, 2017.
- Skj  th, C. A., and Geels, C.: The effect of climate and climate change on ammonia emissions in Europe, *Atmos. Chem. Phys.*, 13, 117-128, doi: 10.5194/acp-13-117-2013, 2013.
- Stockdale, A., Krom, M. D., Mortimer, R. J., Benning, L. G., Carslaw, K. S., Herbert, R. J., Shi, Z., Myriokefalitakis, S., Kanakidou, M., and Nenes, A.: Understanding the nature of atmospheric acid processing of mineral dusts in supplying bioavailable phosphorus to the oceans, *Proceedings of the National Academy of Sciences of the United States of America*, 113, 14639-14644, doi: 10.1073/pnas.1608136113, 2016.
- Surratt, J. D., Chan, A. W., Eddingsaas, N. C., Chan, M., Loza, C. L., Kwan, A. J., Hersey, S. P., Flagan, R. C., Wennberg, P. O., and Seinfeld, J. H.: Reactive intermediates revealed in secondary organic aerosol formation from isoprene, *Proceedings of the National Academy of Sciences of the United States of America*, 107, 6640-6645, doi: 10.1073/pnas.0911114107, 2010.
- Tsimpidi, A. P., Karydis, V. A., and Pandis, S. N.: Response of Inorganic Fine Particulate Matter to Emission Changes of Sulfur Dioxide and Ammonia: The Eastern United States as a Case Study, *J Air Waste Manag. Assoc.*, 57, 1489-1498, doi: 10.3155/1047-3289.57.12.1489, 2007.
- Vasilakos, P., Russell, A., Weber, R., and Nenes, A.: Understanding nitrate formation in a world with less sulfate, *Atmos. Chem. Phys. Disc.*, 1-27, doi: 10.5194/acp-2018-406, 2018.
- Wang, S., Xing, J., Jang, C., Zhu, Y., Fu, J. S., and Hao, J.: Impact assessment of ammonia emissions on inorganic aerosols in East China using response surface modeling technique, *Environ Sci Technol*, 45, 9293-9300, doi: 10.1021/es2022347, 2011.
- Warner, J. X., Dickerson, R. R., Wei, Z., Strow, L. L., Wang, Y., and Liang, Q.: Increased atmospheric ammonia over the world's major agricultural areas detected from space, *Geophys. Res. Lett.*, doi: 10.1002/2016gl072305, 2017.
- Weber, R. J., Guo, H., Russell, A. G., and Nenes, A.: High aerosol acidity despite declining atmospheric sulfate concentrations over the past 15 years, *Nat. Geosci.*, 9, 282-285, doi: 10.1038/ngeo2665, 2016.
- Young, A. H., Keene, W. C., Pszenny, A. A. P., Sander, R., Thornton, J. A., Riedel, T. P., and Maben, J. R.: Phase partitioning of soluble trace gases with size-resolved aerosols in near-surface continental air over northern Colorado, USA, during winter, *J. Geophys. Res.*, 118, 9414-9427, doi: 10.1002/jgrd.50655, 2013.
- Zhang, L., Chen, Y., Zhao, Y., Henze, D. K., Zhu, L., Song, Y., Paulot, F., Liu, X., Pan, Y., Lin, Y., and Huang, B.: Agricultural ammonia emissions in China: reconciling bottom-up and top-down estimates, *Atmos. Chem. Phys.*, 18, 339-355, doi: 10.5194/acp-18-339-2018, 2018.
- Zhu, S., Horne, J. R., Montoya-Aguilera, J., Hinks, M. L., Nizkorodov, S. A., and Dabdub, D.: Modeling reactive ammonia uptake by secondary organic aerosol in CMAQ: application to the continental US, *Atmos. Chem. Phys.*, 18, 3641-3657, doi: 10.5194/acp-18-3641-2018, 2018.

# Effectiveness of Ammonia Reduction on Control of Fine Particle Nitrate

Hongyu Guo<sup>1</sup>, Rene Otjes<sup>2</sup>, Patrick Schlag<sup>3,4,5</sup>, Astrid Kiendler-Scharr<sup>4</sup>, Athanasios Nenes<sup>1,6,7,8</sup>, Rodney J. Weber<sup>1</sup>

<sup>1</sup> School of Earth and Atmospheric Sciences, Georgia Institute of Technology, Atlanta, GA 30332, USA

<sup>2</sup> Energy Research Centre of the Netherlands (ECN), Petten, [the](#) Netherlands

<sup>3</sup> Utrecht University, Utrecht, [the](#) Netherlands

<sup>4</sup> Institute for Energy and Climate Research (IEK-8): Troposphere, Forschungszentrum Jülich, Jülich, Germany

<sup>5</sup> Now at University of Sao Paulo, SP, Brazil

<sup>6</sup> School of Chemical and Biomolecular Engineering, Georgia Institute of Technology, Atlanta, GA 30332, USA

<sup>7</sup> Institute for Chemical Engineering Sciences, Foundation for Research and Technology – Hellas, Patras, GR-26504, Greece

<sup>8</sup> Institute for Environmental Research and Sustainable Development, National Observatory of Athens, P. Penteli, Athens, GR-15236, Greece

\* To whom correspondence should be addressed: [rweber@eas.gatech.edu](mailto:rweber@eas.gatech.edu)

20

**Abstract.** In some regions, reducing aerosol ammonium nitrate ( $\text{NH}_4\text{NO}_3$ ) concentrations may substantially improve air quality. This can be accomplished by reductions in precursor emissions, such as nitrogen oxides ( $\text{NO}_x$ ) to lower nitric acid ( $\text{HNO}_3$ ) that partitions to the aerosol, or reductions in ammonia ( $\text{NH}_3$ ) to lower particle pH and keep  $\text{HNO}_3$  in the gas phase. Using the ISORROPIA-II thermodynamic aerosol model and detailed observational datasets, we explore the sensitivity of aerosol  $\text{NH}_4\text{NO}_3$  to gas phase  $\text{NH}_3$  and  $\text{NO}_x$  controls for a number of contrasting locations, including Europe, the US, and China.  $\text{NO}_x$  control is always effective, whereas the aerosol response to  $\text{NH}_3$  control is highly nonlinear and only becomes effective at a thermodynamic “sweet spot”. The analysis provides a conceptual framework and fundamental evaluation on the relative value of  $\text{NO}_x$  versus  $\text{NH}_3$  control. We find that regardless of the locations examined, it is only when ambient particle pH drops below [an approximate critical value of 3 \(slightly higher in warm and slightly lower in cold seasons\)](#) that  $\text{NH}_3$  reduction leads to an effective response in  $\text{PM}_{2.5}$  mass. The required amount of  $\text{NH}_3$  reduction to efficiently decrease  $\text{NH}_4\text{NO}_3$  at different sites is assessed. Owing to the linkage between  $\text{NH}_3$  emissions and

Deleted: ly

agricultural productivity, substantial  $\text{NH}_3$  reduction required in some locations may not be feasible. Finally, controlling  $\text{NH}_3$  emissions to increase aerosol acidity and evaporate  $\text{NH}_4\text{NO}_3$  will have other effects, beyond reduction of  $\text{PM}_{2.5}$   $\text{NH}_4\text{NO}_3$ , such as increasing aerosol toxicity and potentially altering the deposition patterns of nitrogen and trace nutrients.

**Deleted:** changing



## 1. Introduction

Global trends of increasing gas-phase ammonia ( $\text{NH}_3$ ) concentrations (Erisman et al., 2008) have multiple environmental implications. As part of the global nitrogen cycle (Fowler et al., 2013), excessive  $\text{NH}_3$  deposition promotes alga blooms, degrades water quality, and may be toxic for ecosystems (Krupa, 2003; Camargo and Alonso, 2006).  $\text{NH}_3$  is one of the most important atmospheric alkaline species, as it influences the pH of clouds, fogs, precipitation (Wells et al., 1998), and fine particles ( $\text{PM}_{2.5}$ ) (Guo et al., 2017c). Agricultural practices, including use of synthetic nitrogen-based fertilizer and domesticated animal manure are the major anthropogenic  $\text{NH}_3$  sources (Galloway et al., 2003; Aneja et al., 2009; Zhang et al., 2018). Minor contributions include biomass burning (e.g., forest fires), fossil fuel combustion, and vehicle catalytic converters (Perrino et al., 2002; Behera et al., 2013). Higher temperatures resulting from global warming can also potentially enhance  $\text{NH}_3$  emissions (Skj  th and Geels, 2013). Given that fertilizer usage supports food production for about half the global population (Erisman et al., 2008),  $\text{NH}_3$  emissions are linked to world population and so expected to increase into the 21st century (Gerland et al., 2014). Compared to the limited regulation of  $\text{NH}_3$  emissions, other anthropogenic air pollutants that are linked to acidic atmospheric species, such as sulfur dioxide ( $\text{SO}_2$ ) and nitrogen oxide ( $\text{NO}_x$ ), are regulated through air quality standards, which accounts for their observed decreasing gas and aerosol concentrations in the U.S. (Hand et al., 2012; Russell et al., 2012; Hidy et al., 2014), western Europe, and China (Warner et al., 2017). Decreasing trends of  $\text{SO}_2$  and  $\text{NO}_x$  emissions are expected to continue on global scales throughout the century (IPCC, 2013). The contrast between increasing  $\text{NH}_3$  and decreasing  $\text{SO}_2$  and  $\text{NO}_x$  leads to changes in aerosol composition and mass concentration.  $\text{NH}_3$  reacts rapidly with the oxidized products of  $\text{SO}_2$  and  $\text{NO}_x$ , sulfuric ( $\text{H}_2\text{SO}_4$ ) and nitric ( $\text{HNO}_3$ ) acids, to form ammonium sulfate ( $(\text{NH}_4)_2\text{SO}_4$ , or other forms such as  $\text{NH}_4\text{HSO}_4$ ,  $(\text{NH}_4)_3\text{H}(\text{SO}_4)_2$ ) and ammonium nitrate ( $\text{NH}_4\text{NO}_3$ ) aerosols, which globally constitute an important fraction of ambient  $\text{PM}_{2.5}$  mass (Kanakidou et al., 2005; Sardar et al., 2005; Zhang et al., 2007). These reaction pathways link  $\text{NH}_3$  to  $\text{PM}_{2.5}$  mass and its subsequent impacts on human health (Pope et al., 2004; Lim et al., 2012; Lelieveld et al., 2015; Cohen et al., 2017) and the climate system (Haywood and Boucher, 2000; Bellouin et al., 2011; IPCC, 2013).

Deleted: G

Deleted: and redistribute  $\text{NH}_3$

Deleted: due to temperature increase

Deleted: s

Deleted: and world

Deleted: are strongly tied to population growthrelated

Deleted: and

Deleted: synchronously and sustainably in

Deleted: emissions of

Deleted: and

Deleted: decreases observed

A number of studies using regional or global scale models have investigated  $\text{NH}_3$  controls as a way to reduce  $\text{PM}_{2.5}$  mass to meet air quality standards (Erisman and Schaap, 2004; Pinder et al., 2007; Pinder et al., 2008; Paulot and Jacob, 2014; Bauer et al., 2016; Pozzer et al., 2017). The fundamental premise is that reducing  $\text{NH}_3$  will increase aerosol acidity (i.e., lower aerosol pH) and prevent the formation of  $\text{NH}_4\text{NO}_3$ , reducing overall  $\text{PM}_{2.5}$  mass. As a secondary effect, lower pH can also reduce the sulfate production rate, such as the in-cloud  $\text{SO}_2$  oxidation by  $\text{O}_3$  (Wang et al., 2011; Cheng et al., 2016; Paulot et al., 2017). Use of large-scale models to assess effectiveness of  $\text{NH}_3$  controls requires good predictions of a range of pertinent emissions and sinks ( $\text{NH}_3$ ,  $\text{NO}_x$ ,  $\text{SO}_2$ , and nonvolatile cations), and accurate representation of their applicable atmospheric chemical processes. Thermodynamic modules in different levels of complexity are then applied to determine sensitivities to the precursors (e.g.,  $\text{NH}_3$ ,  $\text{HNO}_3$ ). In some cases (Pozzer et al., 2017), the aerosol pH is explicitly determined with an embedded thermodynamic model, such as ISORROPIA-II (Fountoukis and Nenes, 2007). Due to the complexities from all these factors, chemical transport model-predicted responses to changing emissions may not align with observations. For example, the sensitivity of  $\text{PM}_{2.5}$  pH in the Community Multiscale Air Quality Modeling System (CMAQ) simulations to the mass of crustal material apportioned to the  $\text{PM}_{2.5}$  size range can have important effects on anticipated responses to these changing emission trends. Vasilakos et al. (2018) have shown that including too much crustal material in  $\text{PM}_{2.5}$  results in a predicted increasing trend in both aerosol pH and concentrations of  $\text{NH}_4\text{NO}_3$ , which is counter to observations (Weber et al., 2016).

Overall, calculating aerosol pH is a more accurate approach that provides a fundamental understanding of the factors controlling  $\text{HNO}_3$ - $\text{NO}_3^-$  partitioning and therefore enables a direct evaluation of different studies. Furthermore, it is also useful to determine aerosol pH since it has broad application to many other important aerosol processes. For instance, pH is a mediator of many heterogeneous chemical processes, including various acid-catalyzed reactions (Jang et al., 2002; Eddingsaas et al., 2010; Surratt et al., 2010), gas-particle partitioning of species other than  $\text{HNO}_3$  and  $\text{NH}_3$ , such as organic acids and halogens (Fridlind and Jacobson, 2000; Young et al., 2013; Guo et al., 2017a; Nah et al., 2018), and solubility of metals and other nutrient species (Meskhidze et al., 2003; Nenes et al., 2011; Longo et al., 2016; Stockdale et al., 2016; Fang et al., 2017).

**Deleted:** of a range

**Formatted:** Subscript

**Formatted:** Subscript

**Deleted:** An important parameter that must be accurately predicted in the model is aerosol pH, which is often done by an embedded thermodynamic model, such as ISORROPIA-II (Fountoukis and Nenes, 2007).

**Deleted:** Calculating

**Deleted:** explicitly

**Deleted:** (e.g.,

**Deleted:**

**Formatted:** Subscript

**Formatted:** Subscript

**Deleted:** )

**Deleted:** Despite the importance of pH, this parameter is often obscured in the regional modeling and not explicitly discussed

In this study, we apply a more direct approach, where measured gas and particle concentrations and the thermodynamic model ISORROPIA-II are used directly in a sensitivity analysis to evaluate the effectiveness of NH<sub>3</sub> emission controls on fine particle mass relative to NO<sub>x</sub> control.

Deleted: use

Deleted: the

Deleted: directly

Contrasts are made between sites that have a wide range in NH<sub>3</sub> concentrations and aerosol composition, with a focus on a one-year dataset collected in Cabauw, the Netherlands (Schlag et al., 2016). This site had year around high NH<sub>3</sub> concentrations (average  $7.3 \pm 6.0 \mu\text{g m}^{-3}$ , ~10 ppbv), with nitrate comprising a significant fraction of the fine particle mass (30% NO<sub>3</sub><sup>-</sup> of PM<sub>1</sub>) and there was a strong seasonal temperature variation. The goal is to establish a transparent and fundamental understanding on when NH<sub>3</sub> emission controls could be an effective way to alter aerosol pH to reduce ammonium nitrate aerosol concentrations, without the use of a full chemical transport model.

Deleted:

## 2. Methods

### 2.1 Sampling sites

**Cabauw:** One-year (July 2012 to June 2013) of online aerosol and gas measurements of inorganic species were made at the Cabauw Experimental Site for Atmospheric Research (CESAR), near the village of Cabauw, the Netherlands. Cabauw is a rural site situated approximately 45 km from the Atlantic Ocean (51.970° N, 4.926° E) and surrounded by agricultural land. Northwestern Europe has fairly high NH<sub>3</sub> concentrations with yearly averages ranging from 1 to 14  $\mu\text{g m}^{-3}$  (median as 4.2  $\mu\text{g m}^{-3}$ ) for the Netherlands in 2013, reported by the Measuring Ammonia in Nature (MAN) network (Lolkema et al., 2015). Satellite-derived 14 years average for the western Europe is 3 ppbv ( $\sim 2.3 \mu\text{g m}^{-3}$ ) (Warner et al., 2017). Cabauw was somewhat higher due to intensive agriculture in the region with observed yearly NH<sub>3</sub> average of  $7.3 \pm 6.0 \mu\text{g m}^{-3}$  (~10 ppbv). Site details, instrumentation, and measurement intercomparisons can be found in Schlag et al. (2016). The data used in this analysis is from a monitor for aerosol and gases (MARGA, Applikon Analytical BV) that was operated by the Energy Research Centre of the Netherlands (ECN). The instrument performs online measurements of soluble inorganic gases collected in a continuously wetted-wall denuder, followed by a steam-condensation system for collection of particles. Both the aqueous samples of gases and particles are measured via ion chromatography (Schaap et al., 2011; Rumsey et al., 2014), including NH<sub>3</sub>, HNO<sub>3</sub>, and HCl, and

Moved (insertion) [1]

Deleted: With high NH<sub>3</sub> concentration, it is somewhat

Deleted: The site conditions are representative of the n

Formatted: Subscript

Deleted: (

Deleted: ,

Deleted: in

Deleted:

Deleted: (

Deleted: ,

Deleted: ),

Deleted: and s

Deleted:

Deleted: (~4 ppbv) of the

Deleted: north

Deleted:

Deleted: (~4

Deleted: , ##ug/m3)

Deleted: , where fertilizer usage is high (Warner et al., 2017)..

Deleted: The

Deleted: (

Deleted: ,

Deleted:

Deleted: in Cabauw was somewhat higher than the area

Moved up [1]: yearly averages (ranging from 1 to 14  $\mu\text{g m}^{-3}$ , median as 4.2  $\mu\text{g m}^{-3}$ ) in the Netherlands in 2013 reported by Measuring Ammonia in Nature (MAN) network (Lolkema et al., 2015) and satellite derived 14 years average (~4 ppbv) of the northwestern Europe (Warner et al., 2017)

Deleted: yearly averages (ranging from 1 to 14  $\mu\text{g m}^{-3}$ , median as 4.2  $\mu\text{g m}^{-3}$ ) in the Netherlands in 2013 reported by Measuring Ammonia in Nature (MAN) network (Lolkema et al., 2015) and satellite derived 14 years average (~4 ppbv) of the northwestern Europe (Warner et al., 2017).

particle phase  $\text{NO}_3^-$ ,  $\text{SO}_4^{2-}$ ,  $\text{Cl}^-$ ,  $\text{NH}_4^+$ ,  $\text{Na}^+$ ,  $\text{K}^+$ ,  $\text{Ca}^{2+}$ ,  $\text{Mg}^{2+}$  alternatively between  $\text{PM}_{10}$  and  $\text{PM}_{2.5}$ .

~~each size sampled hourly (i.e., a two-hour interval for one size; a one-hour interval for gas).~~

Deleted: 1 hour for gases and 1 hour for PM??

Deleted: at one-hour intervals

Measurement uncertainties were below 10% (Schaap et al., 2011). The detection limits were 0.05, 0.10, 0.08, and 0.01  $\mu\text{g m}^{-3}$  for aerosol ions  $\text{NH}_4^+$ ,  $\text{NO}_3^-$ ,  $\text{SO}_4^{2-}$ , and  $\text{Cl}^-$ , respectively, and 0.10 and 0.05  $\mu\text{g m}^{-3}$  for the gases  $\text{HNO}_3$  and  $\text{NH}_3$  (Rumsey et al., 2014). Relative humidity (RH) and temperature (T) data were collected at the 2 m level from the CESAR tower and used to represent ground level meteorological conditions (for an overview see Fig. S7 in Schlag et al. (2016)).

**Other Sites:** In addition to the Cabauw site, we analyze the effectiveness of  $\text{NH}_3$  reduction for a number of contrasting sites where we have already reported on aerosol pH in detail. This includes data from the Southern Oxidant and Aerosol Study (SOAS) (Guo et al., 2015), Wintertime Investigation of Transport, Emissions, and Reactivity (WINTER) (Guo et al., 2016), and California Research at the Nexus of Air Quality and Climate Change (CalNex) study (Guo et al., 2017a). Briefly, the SOAS data was collected at the Southeastern Aerosol Research and Characterization (SEARCH) Centerville ground site, representative of the southeastern US background conditions, from June to July 2013. The WINTER data was sampled from the National Center for Atmospheric Research (NCAR) C-130 aircraft operating from Feb to March 2015 mainly in the northeastern US. The CalNex data was collected from May to June 2010 in Pasadena, California, an urban site that is part of the greater Los Angeles region. As a further contrast for regions of very high  $\text{NH}_3$  concentrations, we include an analysis from published data in Beijing during winter haze events in 2015 (Wang et al., 2016), for which pH has also been investigated (Guo et al., 2017c). Table S1 summarizes the conditions at the various sites.

## 2.2 Thermodynamic modeling

The thermodynamic model ISORROPIA-II (Fountoukis and Nenes, 2007) was used to determine the composition and phase state of an  $\text{NH}_4^+$ ,  $\text{SO}_4^{2-}$ ,  $\text{NO}_3^-$ ,  $\text{Cl}^-$ ,  $\text{Na}^+$ ,  $\text{Ca}^{2+}$ ,  $\text{K}^+$ ,  $\text{Mg}^{2+}$ , and water inorganic aerosol and its partitioning with corresponding gases. Thermodynamic equilibrium is assumed between fine particles and gases for all semivolatile inorganic species, including particle water and water vapor. Time scales for submicron particles to reach equilibrium are about 30 minutes (Dassios and Pandis, 1999; Cruz et al., 2000; Fountoukis et al., 2009). The model is run in “forward mode” to calculate gas-particle equilibrium concentrations based on the

input of total concentration of inorganic species (e.g.,  $\text{NH}_3 + \text{NH}_4^+$ ,  $\text{HNO}_3 + \text{NO}_3^-$ ,  $\text{SO}_4^{2-}$ ,  $\text{Na}^+$ ).  $\text{SO}_4^{2-}$  has no gas pair as it is virtually nonvolatile in the observed temperature ranges of this study (An et al., 2007). The forward mode gives more accurate and robust results than reverse mode since it is much less sensitive to measurement uncertainties (Hennigan et al., 2015).

5 Inorganic ions are also assumed to be only in the aqueous phase (i.e., no solid precipitates). This entails a number of assumptions. First, the ambient RH and the history of the particles exposure to RH result in a deliquesced particle. In many cases, diurnal swings in RH (i.e., the maximum RH in early morning) are generally sufficient to reach the deliquescent point. Furthermore, efflorescence RHs are generally low and rarely reached by the ambient RH (10 to 30%) (Bertram et al., 2011). Thus, a deliquesced particle is often a good assumption when average ambient RH is above 50%. For Cabauw, the one-year mean RH was  $81 \pm 15\%$  ( $\pm$  SD), with RH reaching up to 90% during diurnal cycles (see Fig. S1a in the supplement) making the presence of liquid phase a reasonable assumption. For the other sites studied, average RHs were all above 55% (Table S1). A second assumption is that most ions are in an aqueous liquid inorganic phase and only minor fractions reside dissolved in a separate liquid organic phase, if it exists. This is supported by very good agreement between observed ammonia gas-particle partitioning with thermodynamic model predictions that do not consider an organic phase. (See Figs. S3 and S4 for this study; similar results are found in other studies (Guo et al., 2015; Guo et al., 2017a; Nah et al., 2018)). Pye et al. (2018) found only minor difference in predicted ammonia partition when an organic phase was considered. It is also assumed that the particles were internally mixed, and that pH did not vary with size. Mixing state of the nonvolatile cations can affect particle composition and pH (Zhu et al., 2016), but the effect on predicted fine particle pH is small if a minor fraction of nonvolatile sulfate is internally mixed with the nonvolatile cations (Guo et al., 2017b), however, it can add uncertainty to predicted nitric acid partitioning (discussed below in Section 2.3). Since there is no data on the mixing state and the mass concentrations (or mole fractions) of nonvolatile cations are generally small (discussed below in Section 3.2 and also see Table S1), internal mixing is assumed in the following analysis.

With increasing pH (e.g., above 2 for oxalate), organic acids can be found at increasing quantities in the particle phase (Nah et al., 2018). However, organic acids are not considered in the ISORRPIA-II pH calculations. In Cabauw, it has been reported that excess  $\text{NH}_4^+$  (i.e.,  $\text{NH}_4^+$  not paired with  $\text{SO}_4^{2-}$ ,  $\text{NO}_3^-$  and  $\text{Cl}^-$ ) was correlated with (di-)carboxylic organic acids. Excess

Deleted: S2

Deleted: S3

Deleted: (Gao et al., 2016; Gao et al., 2017a; Nah et al., 2018)

Deleted: Pye et al. (2018)

Deleted: also

Deleted: predictions

Deleted: ,

$\text{NH}_4^+$  on average constituted only 5% of the  $\text{NH}_4^+$  reported by an aerosol mass spectrometer (AMS) so it is likely to have a small effect on predicted pH (Schlag et al., 2017). This is confirmed by the good agreement between measured and ISORROPIA-II predicted  $\text{NH}_3$ - $\text{NH}_4^+$  partitioning without considering organic acids or other organic species (see section 3.2).

Deleted: (Schlag et al., 2017)

Deleted: 1

Deleted: ;

5 Although recent modeling study has suggested that ambient  $\text{NH}_3$  concentration can be decreased by as much as 31% in winter and 67% in summer in the US, due to the reactive uptake of  $\text{NH}_3$  by secondary carbonyl compounds (Zhu et al., 2018), this process doesn't appear to have an impact on  $\text{NH}_3$ - $\text{NH}_4^+$  partitioning and predicted pH for the locations in this study. For the winter haze condition in Beijing, the highest pH among the sampling sites, including organic acids (i.e., oxalate) are reported to decrease pH by at most 0.07, therefore a minor effect (Song et al., 2018).

### 2.3 $\text{NO}_x$ vs $\text{NH}_3$ control to limit $\text{PM}_{2.5}$ ammonium nitrate?

Following the various assessments of  $\text{NH}_3$  control on  $\text{PM}_{2.5}$  mass (Erisman and Schaap, 2004; Pinder et al., 2007; Pinder et al., 2008; Paulot and Jacob, 2014; Bauer et al., 2016; Pozzer et al., 2017), we assume the  $\text{PM}_{2.5}$  inorganic nitrate is mainly in the form of semivolatile ammonium

15 nitrate and negligible in nonvolatile forms, such as  $\text{Ca}(\text{NO}_3)_2$ ,  $\text{NaNO}_3$ , and similar species, which are generally not found to a large extent in particles smaller than 1  $\mu\text{m}$ . However, it is noted that in locations where concentrations of minerals or sea-salt particle components are high, and the aerosol has aged, formation of semivolatile  $\text{NH}_4\text{NO}_3$  will be perturbed as the  $\text{HNO}_3$  will evolve over time to the more stable largely coarse mode salts (e.g.,  $\text{CaCl}_2$  and  $\text{NaCl}$ ) at the expense of fine mode  $\text{NH}_4\text{NO}_3$  (see Guo et al. (2017a) for example).

Deleted: neglect

Aerosol organic nitrate species can also contribute to aerosol mass (Farmer et al., 2010; Perring et al., 2013; Xu et al., 2015), and may respond to  $\text{NO}_x$  control, but are not considered here. For the one-year Cabauw data set analyzed here, 9% of the aerosol nitrate was inferred to be organic nitrate, calculated from the difference in Aerosol Chemical Speciation Monitor (ACSM) nitrate and MARGA-measured nitrate (Schlag et al., 2016). Higher fractions (34% to 44%) have been reported for European submicron aerosols (Kiendler-Scharr et al., 2016).  $\text{NO}_x$  emission controls could lead to a change in the relative importance of inorganic and organic nitrate (Edwards et al., 2017).

Focusing just on ammonium nitrate, there are two fundamental ways to control  $\text{PM}_{2.5}$  nitrate; limit the precursors of nitrate aerosol, that is  $\text{HNO}_3$ , or move the nitrate out of the aerosol by

reducing the aerosol pH (increasing the particle acidity). The equilibrium aerosol nitrate concentration is given by:

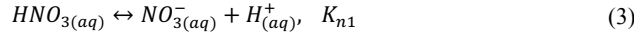
$$NO_3^- = \epsilon(NO_3^-) \times NO_3^T \quad (1)$$

where  $NO_3^-$  is the concentration in air of semivolatile aerosol nitrate and  $\epsilon(NO_3^-)$  is the fraction of  $NO_3^-$  in the particle phase relative to gas plus particle nitrate ( $HNO_3 + NO_3^-$ ), which is defined as total nitrate,  $NO_3^T$ . Eq. (1) is the definition of  $\epsilon(NO_3^-)$ . Because  $\epsilon(NO_3^-)$  depends on pH, the premise of  $NH_3$  control is to reduce  $\epsilon(NO_3^-)$  through decreasing particle pH, whereas  $NO_x$  emission controls will mainly reduce  $NO_3^T$ , although this can also slightly affect pH through aerosol water uptake (discussed below; see Fig. 4 for example).

**$NO_x$  Control:** Emitted  $NO_x$  can undergo a variety of reactions that produce a range of compounds ( $NO_x$ ), including  $HNO_3$ , peroxyntiric acid ( $HO_2NO_2$ ), the nitrate radical ( $NO_3$ ), nitrous acid ( $HONO$ ), dinitrogen pentoxide ( $N_2O_5$ ), and both gas (e.g., PAN) and particle phase nitrate and organic nitrate species. Once gas phase  $HNO_3$  or particle phase  $NO_3^-$  is formed, equilibrium between the phases will re-establish gas and particle concentrations.  $HNO_3$  is largely formed by  $NO_2$  reaction with the hydroxyl radical ( $OH$ ), and at night through the nitrate radical- $N_2O_5$  pathway. Modeling studies show that  $HNO_3$  can be the most significant of  $NO_x$  species (Atkinson, 2000) and is correlated to  $NO_x$  emissions (Shah et al., 2018). Here we assume, to a first approximation, that  $NO_x$  mainly produces  $HNO_3$  (either directly through reaction with  $OH$  or indirectly through production of  $N_2O_5$ ) that partitions to the particle to form semivolatile aerosol nitrate and rapidly reaches equilibrium.  $NO_3^T$  concentrations are then directly related to  $NO_x$  control. Use of more detailed modeling approaches can better assess the relationship between  $NO_x$  emissions and  $NO_3^T$ . For example, we are not considering competing chemical pathways that lead to organic nitrates, versus inorganic nitrate that is in equilibrium with gas phase  $HNO_3$ .

**$NH_3$  Control:** The effectiveness of ammonia control in reducing  $NH_4NO_3$  burdens depends on  $\epsilon(NO_3^-)$  and how it varies with pH, actual pH of the ambient aerosol, and the sensitivity of ambient aerosol pH to changes in  $NH_3$  concentration. From thermodynamic equilibrium,  $\epsilon(NO_3^-)$  can be derived from the solubility, reaction (2), and dissociation, reaction (3), of  $HNO_3$ :





Assuming the solution is ideal,  $\epsilon(\text{NO}_3^-)$  as a function of pH can be predicted solely based on known properties of  $\text{HNO}_3$ ; the  $\text{HNO}_3$  Henry's constant,  $H_{\text{HNO}_3}$ , and the acid dissociation constant,  $K_{n1}$  ( $H_{\text{HNO}_3}$  and  $K_{n1}$  are T dependent), ambient T, and particle liquid water content. The latter is often estimated by only considering water associated with inorganic species ( $W_i$ ;  $\mu\text{g m}^{-3}$ ), determined from measured inorganic aerosol components and relative humidity (RH). Liquid water associated with organic species can also be included, but normally have minor influence on pH of much lower hygroscopicity and the logarithmic nature of pH (Guo et al., 2015). A more accurate result may be achieved by using measured particle water concentrations.

By combining the equilibrium of reactions (2) and (3):

$$\epsilon(\text{NO}_3^-) = \frac{H_{\text{HNO}_3}^* W_i R T (0.987 \times 10^{-14})}{\gamma_{\text{NO}_3^-} \gamma_{\text{H}^+} 10^{-\text{pH}} + H_{\text{HNO}_3}^* W_i R T (0.987 \times 10^{-14})} \quad (4)$$

where  $0.987 \times 10^{-14}$  is a unit conversion factor (from converting atm and  $\mu\text{g}$  to SI units),  $R$  ( $\text{J mol}^{-1} \text{K}^{-1}$ ) is the gas constant and  $H_{\text{HNO}_3}^* = H_{\text{HNO}_3} K_{n1}$  ( $\text{mol}^2 \text{kg}^{-2} \text{atm}^{-1}$ ) is the combined molality-based equilibrium constant of  $\text{HNO}_3$  dissolution and deprotonation, and  $\gamma$  are activity coefficients (equal to 1 if assuming an ideal solution). Derivation of Eq. (4) and references for the temperature dependent equilibrium constants, and similar equations for  $\text{NH}_3$  and  $\text{HCl}$  partitioning, can be found in the supplemental material of Guo et al. (2017a).

### 3. Results and Discussions

#### 3.1 The nitrate partitioning S Curve

The S curve given by Eq. (4) provides a conceptual basis for the effect of ammonia control, through changes in aerosol pH, on particle nitrate. Fig. 1 shows the characteristic “S-shaped” curve of  $\epsilon(\text{NO}_3^-)$  plotted as a function of pH using Eq. (4), for the yearly average conditions in Cabauw and with activity coefficients extracted from ISORROPIA-II ( $\gamma_{\text{NO}_3^-} \gamma_{\text{H}^+} = 0.24$ ).

Including non-ideality shifts the  $\epsilon(\text{NO}_3^-)$  S curve to lower pH by approximately 0.6 units (shown as Fig. S2 in the supplement).

Deleted: .



Fig. 1 shows that there are 3 pertinent pH regions: 1) low pH, where  $\epsilon(\text{NO}_3^-)$  asymptotically approaches 0, and practically all  $\text{NO}_3^-$  is in the gas phase, 2)  $\epsilon(\text{NO}_3^-)$  varies between approximately 0 and 1 and is highly sensitive to pH variations, and, 3) higher pH, where  $\epsilon(\text{NO}_3^-)$  approaches 1 and practically all  $\text{NO}_3^-$  is in the particle phase. This demonstrates that for the one-year average conditions in Cabauw, there is a certain range in ambient pH where  $\text{NH}_3$  control to alter ambient pH will result in a change in  $\text{NO}_3^-$  (i.e., region (2) where pH is between 0 and 3). The greatest change in  $\text{NO}_3^-$  to a lowering of pH occurs when  $\epsilon(\text{NO}_3^-)$  is near 50% (referred to as  $\text{pH}_{50}$ ).

It follows that  $\text{NH}_3$  control will only lead to reduction in  $\text{NO}_3^-$  if ambient particle pH is within region (2) of Fig. 1. If pH is in region (1) there is no need for  $\text{NH}_3$  control since pH is sufficiently low that little  $\text{NO}_3^-$  exists, and if pH is in region (3) the sensitivity of pH to reducing  $\text{NH}_3$  will determine the effectiveness of  $\text{NH}_3$  controls. For example,  $\text{NH}_3$  first needs to be reduced to move particle pH to the transition point between region (2) and (3), where  $\epsilon(\text{NO}_3^-)$  starts to drop. (Note that  $\text{NH}_3$  control also affects particle mass by changing  $\text{NH}_4^+$  concentrations, this is discussed more below [in Section 3.4.](#))

The S curve of Fig. 1 applies for a given situation (see Eq. (4)), which changes as the particle composition or ambient conditions (RH, T) change. For example, if  $\text{NH}_3$  concentrations change, the inorganic particle composition changes, which affects particle water and activity coefficients in Eq. (4), resulting in a shift in the  $\epsilon(\text{NO}_3^-)$  curve. Thus, these curves provide only a sense of the general state of how  $\text{NO}_3^-$  responds to changes in  $\text{NH}_3$ . A full thermodynamic model needs to be run to actually determine the new  $\epsilon(\text{NO}_3^-)$  when conditions change. This analysis is provided in the later part of the paper. The S curve, however, provides valuable insight on sensitivity of  $\epsilon(\text{NO}_3^-)$  to pH for a given situation (i.e., what region of Fig. 1).

### 3.2 pH predicted in Cabauw

High concentrations of aerosol inorganic species were observed during the one-year of observations at the CESAR tower. The mass fractions of  $\text{NO}_3^-$ ,  $\text{SO}_4^{2-}$ ,  $\text{NH}_4^+$ , and  $\text{Cl}^-$  were on average 30%, 15%, 14%, and 1%, respectively, of the  $9.5 \mu\text{g m}^{-3}$  particle mass ( $\text{PM}_{10}$ ) (Schlag et al., 2016). The gas-particle partitioning of three semivolatile pairs,  $\text{NH}_3$ - $\text{NH}_4^+$ ,  $\text{HNO}_3$ - $\text{NO}_3^-$ ,  $\text{HCl}$ - $\text{Cl}^-$ , measured with MARGA are compared with the thermodynamic model predictions (see

Deleted: PM<sub>1</sub>  
Deleted: 2.5  
Deleted: S2  
Deleted: S3

Deleted: S2  
Deleted: , h  
Deleted: ),

Deleted: ,

Deleted: S2  
Deleted: S3  
Deleted: (Guo et al., 2015),  
Deleted: with higher pH of 3.9 at night

section 2 in supplemental material for plots). PM<sub>2.5</sub> and PM<sub>1</sub> MARGA data sets produce similar results (Fig. S3 versus Fig. S4); here we mainly discuss predictions based on PM<sub>2.5</sub>. Measured and ISORROPIA-predicted partitioning of ammonia was in agreement (NH<sub>3</sub>: slope = 1.02, R<sup>2</sup> = 0.997; NH<sub>4</sub><sup>+</sup>: slope = 0.97, R<sup>2</sup> = 0.96) (Fig. S3). NO<sub>3</sub><sup>-</sup> (slope = 1.01, R<sup>2</sup> = 0.987) and Cl<sup>-</sup> (slope = 0.98, R<sup>2</sup> = 0.91) were also in agreement. However, for unknown reasons, gas-phase components of these two species showed significant discrepancies (R<sup>2</sup> of 0.13 to 0.17). We note that it may be associated with the very low gas phase concentrations of these species, in contrast to NH<sub>3</sub>. HNO<sub>3</sub>-NO<sub>3</sub><sup>-</sup> and HCl-Cl<sup>-</sup> were dominated by particle phases,  $\epsilon(\text{NO}_3^-) = \text{NO}_3^-/\text{NO}_3^{\text{T}} = 88 \pm 11 \%$  and  $\epsilon(\text{Cl}^-) = \text{Cl}^-/(\text{Cl}^- + \text{HCl}) = 66 \pm 33 \%$ . The opposite was found for NH<sub>3</sub>-NH<sub>4</sub><sup>+</sup>, the gas-phase dominated with  $\epsilon(\text{NH}_4^+) = \text{NH}_4^+/\text{NH}_x = 19 \pm 15 \%$  (total ammonium is referred to NH<sub>x</sub> = NH<sub>3</sub> + NH<sub>4</sub><sup>+</sup>), which is consistent with particle artifacts in the gas collection system possibly affecting HNO<sub>3</sub> and HCl, but less effect on NH<sub>3</sub>. Furthermore, a generally better prediction of NH<sub>3</sub>-NH<sub>4</sub><sup>+</sup> compared to HNO<sub>3</sub>-NO<sub>3</sub><sup>-</sup> and HCl-Cl<sup>-</sup> partitioning has been observed in our previous studies (Guo et al., 2017a) and is consistent with the lack of a coarse mode sink for NH<sub>3</sub>, in contrast to HNO<sub>3</sub> and HCl, which can react with sodium and other nonvolatile cations and bias the equilibrium states between fine particles and gases. In summary, all the semi-volatile inorganic species in the particle-phase (NO<sub>3</sub><sup>-</sup>, NH<sub>4</sub><sup>+</sup>, and Cl<sup>-</sup>) are predicted with high accuracy, as well as NH<sub>3</sub>-NH<sub>4</sub><sup>+</sup> partitioning, therefore, particle water and pH predictions by ISORROPIA-II are expected to be reasonable.

As noted above, the presence of water-soluble nonvolatile cations (NVCs, here include Na<sup>+</sup>, K<sup>+</sup>, Ca<sup>2+</sup>, Mg<sup>2+</sup>) can affect the bulk pH analysis. In Cabauw, NVC effects can be assessed by comparing hourly PM<sub>1</sub> and PM<sub>2.5</sub> data, since these mechanically generated species are largely found in particles larger than 1 μm diameter. Average NVC mole fractions (i.e., NVCs divided by the total inorganic species, not including liquid water), were consistently small, 5.7% for PM<sub>1</sub> and 5.9% for PM<sub>2.5</sub>. However, Na<sup>+</sup> was slightly higher in PM<sub>2.5</sub> at 0.14 ± 0.25 μg m<sup>-3</sup>, compared to 0.05 ± 0.09 μg m<sup>-3</sup> for PM<sub>1</sub>. The small and nearly identical fractions of NVCs result in the same predicted pH for PM<sub>1</sub> and PM<sub>2.5</sub>; in both cases pH = 3.7 ± 0.6. Therefore, we focus on the PM<sub>2.5</sub> in the following discussion due to the similar partitioning predictions and pH for PM<sub>1</sub> and PM<sub>2.5</sub> (Fig. S3 and S4). A diurnal pattern of ambient particle pH is observed in Cabauw, similar to other studies (Guo et al., 2015). For example, for the nighttime period from 1am to 7am, the

average pH is 3.9, whereas for the daytime period of 1 pm to 6 pm, the pH is ~3.5. The difference is mainly driven by the diurnal variation in liquid water content (see Fig. S1).

Deleted: and lower daytime pH at about 3.5

Deleted: ,

### 3.3 Contrasts in pH and $\epsilon(\text{NO}_3^-)$ between studies

Fig. 2 includes a comparison of  $\epsilon(\text{NO}_3^-)$  versus pH for the different locations and seasons (Fig. S5 shows separate plots for each region). The  $\epsilon(\text{NO}_3^-)$  curves are plotted based on the campaign average conditions (i.e.,  $T$ ,  $W_i$ , and  $\gamma_{\text{NO}_3^-} - \gamma_{\text{H}^+}$ ; all listed in Table S1). Two sub data sets in Cabauw, summer (June-Aug 2012) and winter (Dec 2012-Feb 2013), are shown together with the one-year whole data set. As seen for Cabauw, lower temperatures (dark blue vs. red vs. orange lines in Fig. 2) shifts  $\text{HNO}_3$ - $\text{NO}_3^-$  partitioning to favor the particle phase due to effect of  $T$  on nitric acid Henry's law and dissociation constants, and the explicit effect of  $T$  in Eq. 4. For example, at given activity coefficients and liquid water levels, a decrease from 20 °C (~summer) to 0 °C (~winter) shifts  $\epsilon(\text{NO}_3^-)$  to lower pH by roughly one unit. The differences between the  $\epsilon(\text{NO}_3^-)$  curves are also caused by variations in liquid water, and to a lesser degree by variation in activity coefficients. In general, the summer curves (the right three curves) are at higher pH and the winter curves are at lower pH.

Deleted: S4

In addition to the S curves, Fig. 2 shows the average ambient particle pH predicted by ISORROPIA-II for each of the studies. Note that pH could also be inferred from the S curve and measured  $\epsilon(\text{NO}_3^-)$  but is more uncertain and requires activity coefficients for non-ideality effects. A comparison between Eq. (4)-predicted  $\epsilon(\text{NO}_3^-)$  versus pH and observed  $\epsilon(\text{NO}_3^-)$  versus

Formatted: Highlight

ISORROPIA-predicted pH is shown in Fig. S6 and confirms consistency between the ISORROPIA-predicted pH and S curve given by Eq. (4). (A plot of  $\epsilon(\text{NH}_4^+)$  vs pH is also shown in Fig. S6). Fine ambient particle pH varies amongst the sites. The pH of  $3.7 \pm 0.6$  in Cabauw is higher than several other regions, such as the SE US ( $\text{pH} = 0.9 \pm 0.6$ ), the NE US ( $0.8 \pm 1.0$ ), and the SW US ( $1.9 \pm 0.5$ ), but slightly lower than the China haze ambient particle pH of 4.2. The

Deleted: -II

Deleted:

Deleted: S5

Deleted: S5

higher ambient particle pH is generally associated with higher concentrations of  $\text{NH}_3$  and  $\text{NO}_3^-$ . Particle pH is affected by coupling between many variables, hence the need for a thermodynamic model. ISORROPIA-II predicts the overall resulting equilibrium values and associated pH. Particle nitrate has a secondary effect on pH by increasing particle liquid water and diluting  $\text{H}^+$  aqueous concentrations, resulting in slightly higher pH. This effect is less pronounced when  $\text{SO}_4^{2-}$  levels exceed  $\text{NO}_3^-$ , meaning that liquid water is mainly controlled by nonvolatile  $\text{SO}_4^{2-}$ .

Deleted: Beijing

Thus,  $\text{NH}_3$ ,  $\text{NO}_3^-$ , and particle pH are coupled. Regions of higher  $\text{NH}_3$  will have higher pH which can lead to higher  $\text{NO}_3^-$  (when in Region (2) of Fig. 1). The highest observed  $\text{NH}_3$  ( $12.8 \mu\text{g m}^{-3}$ ) and  $\text{NO}_3^-$  ( $26 \mu\text{g m}^{-3}$ ) concentrations were found for the Beijing haze condition. The Cabauw one-year average  $\text{NH}_3$  was lower at  $7.3 \mu\text{g m}^{-3}$ , and  $\text{NO}_3^-$  was on average of  $4.7 \mu\text{g m}^{-3}$ . The lowest  $\text{NH}_3$  and  $\text{NO}_3^-$  levels were observed in the US studies. For example,  $1.37 \mu\text{g m}^{-3}$   $\text{NH}_3$  and  $3.58 \mu\text{g m}^{-3}$   $\text{NO}_3^-$  in the SW US, and only  $0.39 \mu\text{g m}^{-3}$   $\text{NH}_3$  and  $0.08 \mu\text{g m}^{-3}$   $\text{NO}_3^-$  in the SE US, both in summer.

The intersection of the  $\epsilon(\text{NO}_3^-)$  S curves with ambient particle pH in Fig. 2 (i.e., intersection of vertical line and corresponding site S curve), provide contrast in the average  $\epsilon(\text{NO}_3^-)$  at each site, and hence if how much  $\text{NH}_3$  control will be needed to shift  $\epsilon(\text{NO}_3^-)$  to 50% and corresponding pH of  $\text{pH}_{50}$ . The lowest  $\epsilon(\text{NO}_3^-)$  was found in the SE US at 22% in summer and a higher  $\epsilon(\text{NO}_3^-)$  in the NE US in winter at 39%. The Cabauw site also had higher  $\epsilon(\text{NO}_3^-)$  in winter (91%) than summer (84%). Additionally, the SW US site observed on average 54%  $\epsilon(\text{NO}_3^-)$  in summer and China haze in winter had  $\sim 100\%$   $\epsilon(\text{NO}_3^-)$ . These data show that in the SE US in summer,  $\epsilon(\text{NO}_3^-)$  is generally so low that shifting pH by changing  $\text{NH}_3$  emissions will not greatly influence  $\text{NH}_4\text{NO}_3$  concentrations since most is already in the gas phase. Higher  $\text{NH}_3$  can increase  $\text{NH}_4\text{NO}_3$ , but large changes in  $\text{NH}_3$  are needed in these regions to change pH (Weber et al., 2016). For the SW US summer,  $\text{NO}_3^-$  partitioning is sensitive to changes in pH with a 54%  $\epsilon(\text{NO}_3^-)$ . In Beijing winter, substantial decrease in pH is needed to evaporate  $\text{NH}_4\text{NO}_3$ , even more so than Cabauw in winter. For Cabauw, a substantial reduction in ambient pH would be needed to evaporate  $\text{NO}_3^-$  since the current pH is on the flat zone of the S curve (Region 3), where  $\epsilon(\text{NO}_3^-)$  is near 100%. In summer, however, a much smaller reduction in ambient particle pH would result in a decrease in  $\text{NO}_3^-$ .

### 3.4 Simulation of particle mass reduction with a thermodynamic model

#### 3.4.1 Sensitivities of pH and nitrate partitioning to $\text{NH}_3$ concentration

In the above analysis,  $\epsilon(\text{NO}_3^-)$  versus pH curves relative to ambient particle pH are used to provide insight on how  $\epsilon(\text{NO}_3^-)$  is expected to change with small changes in pH. The S curves are based on the average ambient conditions for each time period, and variables, such as particle water and activity coefficients are held constant. But changes in  $\text{NH}_3$  concentration will vary

Deleted: and

Deleted: eastern

Deleted: 54%

aerosol composition, liquid water content and the activity coefficients, which in turn modulates the S curve, Eq. (4). To address this, in the following analysis, we run ISORROPIA-II for various input  $\text{NH}_x$  concentrations, while T, RH,  $\text{NO}_3^-$  and  $\text{SO}_4^{2-}$  are held constant, and plot various parameters of interest. This takes into account the various aerosol composition and gas phase species concentrations through considering the partitioning of all semi-volatile species, including water, and how this affects thermodynamic properties, such as activity coefficients.

First, we consider the extent of  $\text{NH}_3$  control needed to reduce  $\text{NH}_4\text{NO}_3$ , which depends on the response of pH to changes in ambient  $\text{NH}_3$  concentration, which in turn is related to  $\text{NH}_3$  emissions (i.e., changes in  $\text{NH}_x$ ). In a previous study, we show that for average conditions at the various sites discussed above, a general rule is that an order of magnitude reduction in  $\text{NH}_3$  lowers pH by about one unit (Guo et al., 2017c) ( $\Delta\text{pH}/\Delta(\log_{10}\text{NH}_3)$  are listed in Table S1). At the Cabauw site, the responses in pH to changes in  $\text{NH}_3$  are similar to these other locations; the linear fitted curves for the semi-log plot in Fig. 3a give slopes of 1.00 in winter, 1.16 in summer and 1.05 for the one-year average (all  $R^2 > 0.99$ ). Fig. 3a also shows predicted pH versus measured  $\text{NH}_3$  based on hourly average data. How pH changes with temperature for a constant  $\text{NH}_3$  can also be seen in Fig. 3a; higher temperature leads to lower particle pH due to volatilization of semivolatile  $\text{NH}_4^+$ ,  $\text{NO}_3^-$ , and particle water. The physical explanation for this is that with higher temperature,  $\text{NH}_4^+$  is converted to  $\text{NH}_3$  and releases one  $\text{H}^+$  to the particle phase, whereas  $\text{NO}_3^-$  is converted to  $\text{HNO}_3$  and results in loss of one  $\text{H}^+$  from the particle phase. The former process dominates over the latter due to the differences in temperature dependency of equilibrium constants (see Fig. S7) and the greater loss of  $\text{NH}_4^+$  from  $\text{NH}_4\text{NO}_3$  and  $(\text{NH}_4)_2\text{SO}_4$  compared to less loss of  $\text{NO}_3^-$  only from  $\text{NH}_4\text{NO}_3$ , leading to a net increase in particle  $\text{H}^+$  and lower pH. The loss of water associated with  $\text{NH}_4^+$  and  $\text{NO}_3^-$  further reduces pH, as the  $\text{H}^+$  becomes more concentrated. The water effect is also seen in the diurnal pH trends (see Fig. S1b).

This analysis also permits assessing how  $\varepsilon(\text{NO}_3^-)$ , the sum of  $\text{NH}_4^+$  and  $\text{NO}_3^-$  ( $\text{NH}_4^+ + \text{NO}_3^-$ ), and  $\varepsilon(\text{NH}_4^+)$  responds to changes in  $\text{NH}_3$ . Fig. 3b shows that it takes a factor of 1000 change in  $\text{NH}_3$  concentration ( $\sim 3$  pH units) to reduce  $\varepsilon(\text{NO}_3^-)$  from  $\sim 100\%$  to  $\sim 0\%$  (i.e. from complete particle-phase to complete gas-phase). Also, a change temperature of  $\sim 8^\circ\text{C}$  shifts  $\varepsilon(\text{NO}_3^-)$  equivalent to roughly an order of magnitude change in  $\text{NH}_3$  concentration. (For reference,  $\Delta T$  between winter and one-year averages is  $6.6^\circ\text{C}$  and  $\Delta T$  between one-year average and summer averages is  $8.8^\circ\text{C}$ ). Fig. 3b and 3c again show that larger reductions in  $\text{NH}_3$  are needed in winter compared

Deleted: ,

Deleted: S6

Deleted: 7

Deleted: &

to summer to reduce  $\text{NO}_3^-$ . In Cabauw, only during the highest temperature periods is a  $\text{NH}_3$  control policy immediately effective.

Finally, the response of  $\epsilon(\text{NH}_4^+)$  to changes in  $\text{NH}_3$  is shown in Fig. 3d. The S curves are reversed compared to  $\epsilon(\text{NO}_3^-)$  due to opposite base and acid partitioning responses to changes in pH. Thus, lowering  $\text{NH}_3$  reduces  $\epsilon(\text{NO}_3^-)$ , reducing  $\text{NO}_3^-$  for constant  $\text{NO}_3^{\text{T}}$ , but raises  $\epsilon(\text{NH}_4^+)$  as the particles become more acidic, resulting in relatively more  $\text{NH}_4^+$  in the particle phase and less  $\text{NH}_3$  in the gas phase. This is important since although we discuss  $\text{NH}_3$  emissions, changes in particle pH also affects  $\text{NH}_3$  concentrations through changes in gas-particle partitioning, (i.e.,  $\epsilon(\text{NH}_4^+)$ ), but it is  $\text{NH}_x$  that is really changing through emission controls.

Finally, Fig. 3d shows that temperature has little effect on the  $\epsilon(\text{NH}_4^+)$  versus  $\text{NH}_3$  curves. This is because for constant  $W_i$  and activity coefficients, the  $\epsilon(\text{NH}_4^+)$  versus pH S curves move in the opposite direction with change in temperature than the  $\epsilon(\text{NO}_3^-)$  versus pH S curves;  $\epsilon(\text{NH}_4^+)$  shifts to a lower pH region and  $\epsilon(\text{NO}_3^-)$  shifts to a higher pH region with increasing temperature. This tends to bring the  $\text{NH}_3$ - $\text{NH}_4^+$  partitioning versus  $\text{NH}_3$  curves together and separate the  $\text{HNO}_3$ - $\text{NO}_3^-$  partitioning versus  $\text{NH}_3$  curves for different seasons, considering an increase in pH at lower temperature and constant  $\text{NH}_3$  shown in Fig. 3a or vice versa.

### 3.4.2 Effects of $\text{NH}_3$ , $\text{NO}_x$ , and $\text{SO}_2$ emission control in Cabauw

Here we assess the relative merits of  $\text{NH}_3$ ,  $\text{NO}_x$ , and  $\text{SO}_2$  control on various aspects of  $\text{PM}_{2.5}$  in Cabauw, again using the full thermodynamic model. Changes in pH, particle water ( $W_i$ ),

$\epsilon(\text{NO}_3^-)$ , mass of  $\text{NH}_4^+$  plus  $\text{NO}_3^-$ , and overall  $\text{PM}_{2.5}$  ion mass are assessed when changes are made to  $\text{NH}_x$  ( $\text{NH}_3 + \text{NH}_4^+$ ),  $\text{NO}_3^{\text{T}}$  ( $\text{HNO}_3 + \text{NO}_3^-$ ), and  $\text{SO}_4^{2-}$ , representing control of  $\text{NH}_3$ ,  $\text{NO}_x$ , and  $\text{SO}_2$  emissions, respectively. Each are reduced in steps starting from 0% to a 90% reduction, while holding the other model inputs constant. The results are shown in Fig. 4. The base values are the one-year, summer, and winter average conditions and correspond to 0% reduction in all plots.

The first row in Fig. 4 shows that all parameters respond nonlinearly to  $\text{NH}_x$  reduction, remaining relatively constant until  $\sim 70\%$   $\text{NH}_x$  reduction, at which point they start to rapidly decrease. This is a result of the  $\epsilon(\text{NO}_3^-)$  versus pH S curve of Fig. 1, where little effect is realized until pH reaches a critical value of about 3 (the horizontal dash line in Figs. 4 pH plots). Once

Deleted: (

Deleted: 3c

Deleted: )

Deleted: +

Deleted: a, 4b and 4c

pH drops below this, the balance between  $\text{HNO}_3$  and  $\text{NO}_3^-$  is sharply shifted towards the gas phase due to the combined effects of reduced particle pH and also reduced particle water ( $W_i$ ). An approximate 70% reduction in  $\text{NH}_x$  is required in Cabauw, in winter or based on the yearly average data, to achieve effective reductions in  $(\text{NH}_4^+ + \text{NO}_3^-)$  and particle ion mass. In summer, some minor reductions in the mass concentrations occur for small  $\text{NH}_x$  reductions, since pH is slightly lower in summer (3.3) compared to winter (3.9). Despite the seasonal variations in gas and particle composition, RH and T, all three pH curves (one-year, summer, winter) appear to be similar and show a critical pH of approximate 3;  $\text{NH}_x$  reduction is more effective for pH below 3 but far less effective for pH above 3, consistent with the simplified analysis above (see Fig. 1).

Effects of reducing  $\text{NO}_3^-$  (the 2<sup>nd</sup> row, Fig. 4b, i.e.,  $\text{NO}_x$  control) and  $\text{SO}_4^{2-}$  (the 3<sup>rd</sup> row, i.e.,  $\text{SO}_2$  control) show different responses. For  $\text{NO}_x$  control, holding  $\text{NH}_x$  and  $\text{SO}_4^{2-}$  constant, a linear reduction in  $\text{NO}_3^-$  causes a linear decrease in  $W_i$ ,  $(\text{NH}_4^+ + \text{NO}_3^-)$  and  $\text{PM}_{2.5}$  ion concentrations simply because  $\varepsilon(\text{NO}_3^-)$  remains close to 1 so that  $\text{NO}_3^- \sim \text{NO}_3^T$ . Then a reduction  $\text{NO}_3^T$  is just transmitted directly to  $W_i$  ( $\text{SO}_4^{2-}$  is constant so particle hygroscopicity is controlled by  $\text{NO}_3^-$ ),  $(\text{NH}_4^+ + \text{NO}_3^-)$  and  $\text{PM}_{2.5}$  ions.  $\varepsilon(\text{NO}_3^-)$  is relatively constant (more so in winter) because it is  $\sim 100\%$  and so not sensitive to the changes in  $W_i$ . Lower  $W_i$  does shift the  $\text{HNO}_3$ - $\text{NO}_3^-$  S curve towards a higher pH, but since pH is affected little, and never drops below the critical value of 3,  $\text{HNO}_3$ - $\text{NO}_3^-$  partitioning is barely affected by reducing  $\text{NO}_3^T$  (i.e., remains in Region (3) in Fig. 1).

In the case of  $\text{SO}_4^{2-}$  reduction, particle pH only increases slightly with substantial  $\text{SO}_4^{2-}$  reduction due to buffering by  $\text{NH}_3$ - $\text{NH}_4^+$  partitioning (i.e.,  $\text{NH}_4^+$  volatility) (Weber et al., 2016; Guo et al., 2017c).  $(\text{NH}_4^+ + \text{NO}_3^-)$  decreases slightly due to the loss of associated  $\text{NH}_4^+$  due to both the drop in  $\text{SO}_4^{2-}$  and volatilization caused by reduced particle water. Since  $\text{SO}_4^{2-}$  is nonvolatile and no gas-particle partitioning is involved, the  $\text{SO}_4^{2-}$  reduction results in a linear reduction in particle ionic mass, while model input of  $\text{NH}_x$  and  $\text{NO}_3^T$  are constant.

Sensitivity test were also performed to investigate the robustness of these results. Considering the observed decreasing trends of  $\text{SO}_2$  emissions in many regions (Hand et al., 2012; Hidy et al., 2014; Warner et al., 2017), we tested a cleaner future with less sulfate (20% of the current level, see Fig. S8 in the supplement). Also, since significant changes in global climate and surface land cover can result in a dustier future with more NVCs, we investigated the effect of a 400%

Deleted: S7

increase in NVCs above the Cabauw levels (see Fig. S9). These two assumed scenarios produce a similar conclusion as the base simulation discussed above, including our finding of a critical pH of 3 and nonlinear response to a  $\text{NH}_x$  reduction. We do note, however, that in the reduced  $\text{SO}_4^{2-}$  case,  $\text{SO}_4^{2-}$  control had nearly no effect on particle ion mass because of the very low  $\text{SO}_4^{2-}$  concentrations to begin with in the cleaner future scenario.

Deleted: S8

In summary, the optimal strategy to reduce ammonium nitrate or particle total inorganic ion mass for the current conditions in Cabauw is to control  $\text{NO}_3^-$  ( $\text{NO}_x$  emission) since it results in a linear response. Even  $\text{SO}_4^{2-}$  control is superior over  $\text{NH}_x$  control to reduce particle ion mass, unless over 70% reduction in  $\text{NH}_x$  could be achieved. If  $\text{NH}_x$  is reduced, the effects will be greatest in warmer periods. These are also the times when  $\text{NH}_3$  emissions and concentrations are largest regionally or globally (Yamamoto et al., 1988; Warner et al., 2016; Warner et al., 2017; Zhang et al., 2018) (see Table S1 for Cabauw  $\text{NH}_3$  levels), and so there may be other benefits to controlling  $\text{NH}_3$  emissions at these times, for example, minimizing eutrophication in surface aqueous systems.

Deleted: both in Cabauw (Table S1) and in other regions of generally high  $\text{NH}_3$  concentrations, such as Asia

The above findings in Cabauw are in contrast to results of a global model, which also utilized ISORROPIA-II (Pozzer et al., 2017). They find the impacts of  $\text{NH}_3$  emissions on  $\text{PM}_{2.5}$  mass is strongest in winter for Europe (along with North America, and Asia). Some of the differences are likely attributed to our higher predicted pH in Cabauw of  $\sim 3.7$  compared to the average pH of Europe predicted in the global model to be near 2 (Pozzer et al., 2017). Thus, we predict conditions above the critical pH of 3, and Pozzer et al. (2017) predicts pH below this value. Difference in pH may be due to meteorological conditions or the concentration of aerosol and gas inorganic species, but it does demonstrate the sensitivity of responses to what the local ambient pH is, and that care should be taken to evaluate predicted particle pH against inferences from ambient measurements. Another thermodynamic model may give a different pH compared to ISORROPIA-II, which may result in a slightly different critical pH (i.e.,  $\sim 3$  in this study). Next, we explore the outcomes of  $\text{NH}_x$  reductions in other locations and show that  $\text{NH}_3$  emission control is more effective in winter than summer.

Deleted: . This needs to be considered evaluating

Deleted: the

Deleted: of

Deleted: i

Deleted: f comparing different approaches

### 3.4.3 Effects of $\text{NH}_3$ , $\text{NO}_x$ , and $\text{SO}_2$ emission control for other locations

$\text{NH}_x$ ,  $\text{NO}_3^-$ , and  $\text{SO}_4^{2-}$  reduction tests were also run for the other sampling sites following the same approach as described above for Cabauw. The model input (period averages) can be found



in Table S1 and the results summarized in Fig. 5. The Cabauw simulations are included in Fig. 5 for direct comparison with the other studies, despite being also plotted in Fig. 4. The average fine particle pH and  $\epsilon(\text{NO}_3^-)$  in each study are listed at the top of each plot in Fig. 5 and the plots for the different studies are arranged with increasing ambient pH from left to right. This order is followed in the following discussion.

Fine particles in the eastern US (SOAS and WINTER studies, Fig. 5a and 5b) are the most acidic among the sites, with average pH of approximately 1 due to the lowest  $\text{NH}_3$  (and to some minor extent due to small  $\text{NO}_3^-$ , through its effect on liquid water). In the NE US, in winter,  $\text{NH}_x$  control is most efficient in decreasing  $\text{PM}_{2.5}$  ion mass since the particle pH and  $\epsilon(\text{NO}_3^-)$  (37%) indicate a “sweet spot”, where the change in  $\text{NH}_x$  emission affects  $\text{NO}_3^-$  immediately.  $\text{PM}_{2.5}$  ion mass reductions from  $\text{NO}_3^-$  control and  $\text{SO}_4^{2-}$  control are similar, since aerosol  $\text{NO}_3^-$  and  $\text{SO}_4^{2-}$  are comparable in mass. In the SE US in summer,  $\text{NO}_3^-$  control is not effective because  $\text{NO}_3^-$  only contributed 4% to the  $\text{NH}_4^+$ - $\text{SO}_4^{2-}$ - $\text{NO}_3^-$  aerosols (Fig. 5a). A small fraction of nitrate aerosol is typically observed in the southeast in summer (Hidy et al., 2014), due to the high temperature and low particle pH. Because of the small  $\text{NO}_3^-$  fraction and already low pH in summer,  $\text{NH}_x$  control only leads to minor reductions in particle ionic mass. In contrast,  $\text{SO}_4^{2-}$  control produces the highest reduction of particle ionic mass since it is the dominant inorganic species (76%) in this region. Therefore, it is more effective to control  $\text{NH}_x$  in winter in the NE US and  $\text{SO}_4^{2-}$  in summer in the SE US, a finding consistent with previous studies (Duyzer, 1994; Tsimpidi et al., 2007).

For the southwest US summer (CalNex study, Fig. 5c), since  $\text{NO}_3^-$  was the most abundant among  $\text{NH}_4^+$ - $\text{SO}_4^{2-}$ - $\text{NO}_3^-$  aerosol components, reducing  $\text{NH}_x$  is the most effective way to reduce  $\text{PM}_{2.5}$  ion mass as the ambient particle pH is within the range where  $\epsilon(\text{NO}_3^-)$  is sensitive to pH.  $\text{NO}_3^-$  control follows closely in effectiveness, whereas reducing  $\text{SO}_4^{2-}$  is the least effective. In the WINTER (NE US winter) and CalNex (SW US summer) studies,  $\text{PM}_{2.5}$  ion mass decreases at a lower rate towards higher levels in  $\text{NH}_x$  reduction (see Fig. 5b and 5c) due to the nonlinear response in  $\epsilon(\text{NO}_3^-)$  to  $\text{NH}_3$  concentration (as shown in Fig. 3b or Fig. 2). For instance, when  $\epsilon(\text{NO}_3^-)$  drops from 50% to 0%, the sensitivities to  $\text{NH}_3$  keeps decreasing asymptotically towards zero. The pH stays nearly flat for the  $\text{NO}_3^-$  control and  $\text{SO}_4^{2-}$  control and decreases with  $\text{NH}_x$  control.

Deleted: winter (

Deleted: ),

Deleted: corresponds to a higher

Formatted: Font:Italic

Deleted: in winter than in summer (22%)

Deleted: southeastern

Deleted: The

Deleted: time

Deleted: , owning

Deleted: strong

Deleted: acidity

Deleted: the eastern

Deleted: until reaching

Deleted: 5f

Deleted: 5e

Deleted: 19

Deleted: , as

Deleted: is

Deleted: a

Deleted: Thus, I

Deleted: produces more localized HNO<sub>3</sub> deposition and less localized NH<sub>3</sub> deposition near the NO<sub>x</sub> and NH<sub>3</sub> sources, respectively, since the gases deposit faster than the particle phase.

Cabauw winter and Beijing winter haze conditions (see Fig. 5e and 5f) are similar in terms of benefits in reducing particle ionic mass from NH<sub>x</sub>, NO<sub>3</sub><sup>T</sup>, or SO<sub>4</sub><sup>2-</sup> controls. This is because of similarities in pH and ε(NO<sub>3</sub><sup>-</sup>) between these sites. For the haze condition in Beijing, NH<sub>x</sub> control doesn't produce as much PM<sub>2.5</sub> ion mass reduction as NO<sub>3</sub><sup>T</sup> and SO<sub>4</sub><sup>2-</sup> controls, unless more than a 60% reduction in NH<sub>x</sub> is reached. However, after that PM mass reduction is fast. At 90% NH<sub>x</sub> reduction, a decrease of more than half of the particle ionic mass is predicted. NO<sub>3</sub><sup>T</sup> and SO<sub>4</sub><sup>2-</sup> controls produce equivalent results due to the same mass fractions of NO<sub>3</sub><sup>-</sup> and SO<sub>4</sub><sup>2-</sup> (both equal to 36%) and linear response in particle ionic mass. Comparing the pH profiles, the largest reduction in pH is predicted for Beijing haze if reducing NH<sub>x</sub>. At 50% NH<sub>x</sub> reduction, pH changes from 4.1 to 2.5 in Beijing, whereas pH only changes from 3.9 to 3.3 in Cabauw. This can be explained by differences in ε(NH<sub>4</sub><sup>+</sup>), which is at 60% in Beijing versus 27% in Cabauw.

### 3.5 Other implications of lowering pH by NH<sub>3</sub> emission control

The benefit of reducing NH<sub>3</sub> emission to reduce ambient PM<sub>2.5</sub> mass concentrations depends on the conditions at a specific site. While particle pH is lowered during the process, other pH related atmospheric processes are affected. One potentially unintended effect is nitrogen deposition.

Nitrogen dry deposition rates depend on particle versus gas phase fractions, since there are large differences between gas and particle deposition velocities. For example, the dry deposition velocity of NH<sub>3</sub> is about 1-2 cm s<sup>-1</sup> over forests, agricultural, or mixed-use land, and 10 times that of NH<sub>4</sub><sup>+</sup> (Duyzer, 1994; Schrader and Brummer, 2014). Also, the dry deposition velocity of HNO<sub>3</sub> is similar to that of NH<sub>3</sub> (Huebert and Robert, 1985). Lowering particle pH through NH<sub>3</sub> reductions will decrease overall reduced nitrogen deposition, but may results in more localized oxidized nitrogen dry deposition, if the lower pH results in NO<sub>3</sub><sup>-</sup> evaporation and higher HNO<sub>3</sub> concentrations. Deposition due to wet removal processes are not considered here.

An addition consequence of lowering particle pH is that it can increase aerosol toxicity. Many studies have identified links between strong particle acidity and adverse health endpoints (Koutrakis et al., 1988; Thurston et al., 1994; Raizenne et al., 1996; Gwynn et al., 2000; Lelieveld et al., 2015). We recently showed one way this can happen is due to increased conversion of PM<sub>2.5</sub> insoluble transition metals to soluble forms by strong acidity (Fang et al., 2017), which increases the particles ability to induce oxidative stress (Ghio et al., 2012). Lowering pH may reduce PM<sub>2.5</sub> mass but increase overall potential for adverse health effects due

to significantly greater toxicity of soluble metals relative to ammonium nitrate. Finally, lowering pH can also impact the deposition pattern and bioavailability of trace limiting nutrients such as Fe, P, and other metals (Meskhidze et al., 2003; Nenes et al., 2011) with important implications for primary productivity (Meskhidze et al., 2005) and even the oxygen state of the subsurface ocean (Ito et al., 2016).

#### 4. Summary

In this study, we assess the effectiveness of  $\text{NH}_3$  control as a way to lower inorganic  $\text{PM}_{2.5}$  mass based on observational data sets from the US, the Netherlands, and China during different seasons. These sites encompass a diverse range in  $\text{NH}_3$  and inorganic aerosol concentrations, and thermodynamic conditions. In all cases, the relative humidities are sufficiently high (average  $\text{RH} > 55\%$ ) that a completely deliquesced inorganic phase is a reasonable assumption, which is implicit to the thermodynamic calculations (metastable mode). Focusing on Cabauw, the Netherlands, a site in a region highly impacted by agricultural emissions, we show that the effectiveness of  $\text{NH}_3$  control changes with season. In winter, a much larger reduction in  $\text{NH}_3$  is required to reduce  $\text{NO}_3^-$  than in summer, making  $\text{NO}_x$  control more effective in winter. This is explained by a shift in the  $\text{HNO}_3$ - $\text{NO}_3^-$  partitioning ( $\epsilon(\text{NO}_3^-)$ ) curve to lower pH in winter and  $\text{pH}_{50}$  (where  $\epsilon(\text{NO}_3^-) = 50\%$ ) further from the actual ambient particle pH. A similar situation is seen in Beijing in winter, where  $\text{NH}_3$  emission control would also be less effective. In most other sites investigated,  $\text{NH}_3$  control is effective in reducing  $\text{PM}_{2.5}$  mass, in regions with reasonably high ammonium nitrate concentrations.

The analysis presented here provides a conceptual and direct evaluation of how the inorganic gas-particle system can be expected to respond to changes in  $\text{NH}_3$  emissions, and how it contrasts to  $\text{NO}_x$  control. The approach relies on the single  $\text{HNO}_3$ - $\text{NO}_3^-$  partitioning equation and the use of a thermodynamic model to predict pH. Other approaches are also often used to address this question. Chemical transport models with imbedded thermodynamic sub-modules (such as ISORROPIA) can provide a more detailed analysis that includes other possible impacts of the emission controls, such as ammonia and nitrate deposition and associated environmental impacts. However, the various uncertainties associated with the many simulated processes involved in these models (e.g., emissions and processing) can affect the predicted results and

**Deleted:** and somewhat representative of northwestern Europe,

obscure the fundamental partitioning processes. With the more transparent and accessible approach presented here, this is less an issue. Both approaches have benefits, but whichever analysis is utilized, it is always useful to explicitly report estimated particle pH as it allows assessment of the predictions and provides contrasts between studies at specific sites.

5

## Acknowledgements

This work was supported by the National Science Foundation (NSF) under grant AGS-1360730 and by the US Environmental Protection Agency STAR Grant R835882. This publication's  
 10 contents are solely the responsibility of the grantee and do not necessarily represent the official views of the US EPA. Further, US EPA does not endorse the purchase of any commercial products or services mentioned in the publication. AN acknowledges support from the European Research Council Project PyroTRACH (Pyrogenic TRansformations Affecting Climate and Health) Grant Agreement 726165. [We acknowledge Fred Bosveld \(KNMI\) and the CESAR](#)  
 15 [database \(www.cesar-database.nl\) for sharing the meteorological data.](#)

## References

- An, W. J., Pathak, R. K., Lee, B.-H., and Pandis, S. N.: Aerosol volatility measurement using an improved thermodenuder: Application to secondary organic aerosol, *J. Aerosol Sci.*, 38, 305-314, doi: 10.1016/j.jaerosci.2006.12.002, 2007.
- 20 Aneja, V. P., Schlesinger, W. H., and Erisman, J. W.: Effects of Agriculture upon the Air Quality and Climate: Research, Policy, and Regulations, *Environ. Sci. Technol.*, 43, 4234-4240, doi: 10.1021/es8024403, 2009.
- Atkinson, R.: Atmospheric chemistry of VOCs and NO<sub>x</sub>, *Atmos. Environ.*, 34, 2063-2101, doi: 10.1016/s1352-2310(99)00460-4, 2000.
- 25 Bauer, S. E., Tsigaridis, K., and Miller, R.: Significant atmospheric aerosol pollution caused by world food cultivation, *Geophys. Res. Lett.*, 43, 5394-5400, doi: 10.1002/2016gl068354, 2016.
- Behera, S. N., Sharma, M., Aneja, V. P., and Balasubramanian, R.: Ammonia in the atmosphere: a review on emission sources, atmospheric chemistry and deposition on terrestrial bodies,  
 30 *Environ. Sci. Pollut. Res. Int.*, 20, 8092-8131, doi: 10.1007/s11356-013-2051-9, 2013.
- Bellouin, N., Rae, J., Jones, A., Johnson, C., Haywood, J., and Boucher, O.: Aerosol forcing in the Climate Model Intercomparison Project (CMIP5) simulations by HadGEM2-ES and the role of ammonium nitrate, *J. Geophys. Res.*, 116, D20206, doi: 10.1029/2011jd016074, 2011.

- Bertram, A. K., Martin, S. T., Hanna, S. J., Smith, M. L., Bodsworth, A., Chen, Q., . . . Zorn, S. R.: Predicting the relative humidities of liquid-liquid phase separation, efflorescence, and deliquescence of mixed particles of ammonium sulfate, organic material, and water using the organic-to-sulfate mass ratio of the particle and the oxygen-to-carbon elemental ratio of the organic component, *Atmos. Chem. Phys.*, 11, 10995-11006, doi: 10.5194/acp-11-10995-2011, 2011.
- Camargo, J. A., and Alonso, A.: Ecological and toxicological effects of inorganic nitrogen pollution in aquatic ecosystems: A global assessment, *Environ. Int.*, 32, 831-849, doi: 10.1016/j.envint.2006.05.002, 2006.
- 10 Cheng, Y., Zheng, G., Wei, C., Mu, Q., Zheng, B., Wang, Z., . . . Su, H.: Reactive nitrogen chemistry in aerosol water as a source of sulfate during haze events in China, *Sci. Adv.*, 2, e1601530, doi: 10.1126/sciadv.1601530, 2016.
- Cohen, A. J., Brauer, M., Burnett, R., Anderson, H. R., Frostad, J., Estep, K., . . . Forouzanfar, M. H.: Estimates and 25-year trends of the global burden of disease attributable to ambient air pollution: an analysis of data from the Global Burden of Diseases Study 2015, *Lancet*, 389, 1907-1918, doi: 10.1016/s0140-6736(17)30505-6, 2017.
- 15 Cruz, C. N., Dassios, K. G., and Pandis, S. N.: The effect of dioctyl phthalate films on the ammonium nitrate aerosol evaporation rate, *Atmos. Environ.*, 34, 3897-3905, doi: 10.1016/S1352-2310(00)00173-4, 2000.
- 20 Dassios, K. G., and Pandis, S. N.: The mass accommodation coefficient of ammonium nitrate aerosol, *Atmos. Environ.*, 33, 2993-3003, doi: 10.1016/S1352-2310(99)00079-5, 1999.
- Duyzer, J.: Dry deposition of ammonia and ammonium aerosols over heathland, *J. Geophys. Res.*, 99, 18757-18763, doi: 10.1029/94jd01210, 1994.
- Eddingsaas, N. C., VanderVelde, D. G., and Wennberg, P. O.: Kinetics and Products of the Acid-Catalyzed Ring-Opening of Atmospherically Relevant Butyl Epoxy Alcohols, *J. Phys. Chem. A*, 114, 8106-8113, doi: 10.1021/Jp103907c, 2010.
- 25 Edwards, P. M., Aikin, K. C., Dube, W. P., Fry, J. L., Gilman, J. B., de Gouw, J. A., . . . Brown, S. S.: Transition from high- to low- $\text{NO}_x$  control of night-time oxidation in the southeastern US, *Nat. Geosci.*, 10, 490-495, doi: 10.1038/ngeo2976, 2017.
- 30 Erisman, J. W., and Schaap, M.: The need for ammonia abatement with respect to secondary PM reductions in Europe, *Environ. Pollut.*, 129, 159-163, doi: 10.1016/j.envpol.2003.08.042, 2004.
- Erisman, J. W., Sutton, M. A., Galloway, J., Klimont, Z., and Winiwarter, W.: How a century of ammonia synthesis changed the world, *Nat. Geosci.*, 1, 636-639, 2008.
- 35 Fang, T., Guo, H., Zeng, L., Verma, V., Nenes, A., and Weber, R. J.: Highly Acidic Ambient Particles, Soluble Metals, and Oxidative Potential: A Link between Sulfate and Aerosol Toxicity, *Environ. Sci. Technol.*, 51, 2611-2620, doi: 10.1021/acs.est.6b06151, 2017.
- Farmer, D. K., Matsunaga, A., Docherty, K. S., Surratt, J. D., Seinfeld, J. H., Ziemann, P. J., and Jimenez, J. L.: Response of an aerosol mass spectrometer to organonitrates and organosulfates and implications for atmospheric chemistry, *Proc. Natl. Acad. Sci. U.S.A.*, 107, 6670-6675, doi: 10.1073/pnas.0912340107, 2010.
- 40 Fountoukis, C., and Nenes, A.: ISORROPIA II: a computationally efficient thermodynamic equilibrium model for  $\text{K}^+$ - $\text{Ca}^{2+}$ - $\text{Mg}^{2+}$ - $\text{NH}_4^+$ - $\text{Na}^+$ - $\text{SO}_4^{2-}$ - $\text{NO}_3^-$ - $\text{Cl}^-$ - $\text{H}_2\text{O}$  aerosols, *Atmos. Chem. Phys.*, 7, 4639-4659, doi: 10.5194/acp-7-4639-2007, 2007.

- Fountoukis, C., Nenes, A., Sullivan, A., Weber, R., Van Reken, T., Fischer, M., . . . Cohen, R. C.: Thermodynamic characterization of Mexico City aerosol during MILAGRO 2006, *Atmos. Chem. Phys.*, 9, 2141-2156, doi: 10.5194/acp-9-2141-2009, 2009.
- 5 Fowler, D., Coyle, M., Skiba, U., Sutton, M. A., Cape, J. N., Reis, S., . . . Voss, M.: The global nitrogen cycle in the twenty-first century, *Philos. Trans. R. Soc. B*, 368, 20130164, doi: 10.1098/rstb.2013.0164, 2013.
- Fridlind, A. M., and Jacobson, M. Z.: A study of gas-aerosol equilibrium and aerosol pH in the remote marine boundary layer during the First Aerosol Characterization Experiment (ACE 1), *J. Geophys. Res.*, 105, 17325-17340, doi: 10.1029/2000jd900209, 2000.
- 10 Galloway, J. N., Aber, J. D., Erisman, J. W., Seitzinger, S. P., Howarth, R. W., Cowling, E. B., and Cosby, B. J.: The Nitrogen Cascade, *BioScience*, 53, doi: 10.1641/0006-3568(2003)053[0341:Tnc]2.0.Co;2, 2003.
- Gerland, P., Raftery, A. E., Sevckova, H., Li, N., Gu, D., Spoorenberg, T., . . . Wilmoth, J.: World population stabilization unlikely this century, *Science*, 346, 234-237, doi: 10.1126/science.1257469, 2014.
- 15 Ghio, A. J., Carraway, M. S., and Madden, M. C.: Composition of air pollution particles and oxidative stress in cells, tissues, and living systems, *J. Toxicol. Environ. Health. B Crit. Rev.*, 15, 1-21, doi: 10.1080/10937404.2012.632359, 2012.
- Guo, H., Xu, L., Bougiatioti, A., Cerully, K. M., Capps, S. L., Hite, J. R., . . . Weber, R. J.: Fine-particle water and pH in the southeastern United States, *Atmos. Chem. Phys.*, 15, 5211-5228, doi: 10.5194/acp-15-5211-2015, 2015.
- 20 Guo, H., Sullivan, A. P., Campuzano-Jost, P., Schroder, J. C., Lopez-Hilfiker, F. D., Dibb, J. E., . . . Weber, R. J.: Fine particle pH and the partitioning of nitric acid during winter in the northeastern United States, *J. Geophys. Res.*, 121, 10355-10376, doi: 10.1002/2016jd025311, 2016.
- 25 Guo, H., Liu, J., Froyd, K. D., Roberts, J. M., Veres, P. R., Hayes, P. L., . . . Weber, R. J.: Fine particle pH and gas-particle phase partitioning of inorganic species in Pasadena, California, during the 2010 CalNex campaign, *Atmos. Chem. Phys.*, 17, 5703-5719, doi: 10.5194/acp-17-5703-2017, 2017a.
- 30 Guo, H., Nenes, A., and Weber, R. J.: The underappreciated role of nonvolatile cations on aerosol ammonium-sulfate molar ratios, *Atmos. Chem. Phys. Disc.*, 1-19, doi: 10.5194/acp-2017-737, 2017b.
- Guo, H., Weber, R. J., and Nenes, A.: High levels of ammonia do not raise fine particle pH sufficiently to yield nitrogen oxide-dominated sulfate production, *Sci. Rep.*, 7, doi: 10.1038/s41598-017-11704-0, 2017c.
- 35 Gwynn, R. C., Burnett, R. T., and Thurston, G. D.: A time-series analysis of acidic particulate matter and daily mortality and morbidity in the Buffalo, New York, region, *Environ. Health Perspect.*, 108, 125-133, doi: 10.2307/3454510, 2000.
- Hand, J. L., Schichtel, B. A., Malm, W. C., and Pitchford, M. L.: Particulate sulfate ion concentration and SO<sub>2</sub> emission trends in the United States from the early 1990s through 2010, *Atmos. Chem. Phys.*, 12, 10353-10365, doi: 10.5194/acp-12-10353-2012, 2012.
- 40 Haywood, J., and Boucher, O.: Estimates of the direct and indirect radiative forcing due to tropospheric aerosols: A review, *Rev. Geophys.*, 38, 513-543, doi: 10.1029/1999rg000078, 2000.

- Hennigan, C. J., Izumi, J., Sullivan, A. P., Weber, R. J., and Nenes, A.: A critical evaluation of proxy methods used to estimate the acidity of atmospheric particles, *Atmos. Chem. Phys.*, 15, 2775-2790, doi: 10.5194/acp-15-2775-2015, 2015.
- Hidy, G. M., Blanchard, C. L., Baumann, K., Edgerton, E., Tanenbaum, S., Shaw, S., . . . Walters, J.: Chemical climatology of the southeastern United States, 1999-2013, *Atmos. Chem. Phys.*, 14, 11893-11914, doi: 10.5194/acp-14-11893-2014, 2014.
- Huebert, B. J., and Robert, C. H.: The Dry Deposition of Nitric-Acid to Grass, *J. Geophys. Res.*, 90, 2085-2090, doi: 10.1029/JD090iD01p02085, 1985.
- IPCC: Climate Change 2013: The Physical Science Basis. Contribution of Working Group I to the Fifth Assessment Report of the Intergovernmental Panel on Climate Change., Cambridge, United Kingdom and New York, NY, USA, 1535, 2013.
- Ito, T., Nenes, A., Johnson, M. S., Meskhidze, N., and Deutsch, C.: Acceleration of oxygen decline in the tropical Pacific over the past decades by aerosol pollutants, *Nat. Geosci.*, 9, 443-447, doi: 10.1038/ngeo2717, 2016.
- Jang, M., Czoschke, N. M., Lee, S., and Kamens, R. M.: Heterogeneous atmospheric aerosol production by acid-catalyzed particle-phase reactions, *Science*, 298, 814-817, doi: 10.1126/science.1075798, 2002.
- Kanakidou, M., Seinfeld, J. H., Pandis, S. N., Barnes, I., Dentener, F. J., Facchini, M. C., . . . Wilson, J.: Organic aerosol and global climate modelling: a review, *Atmos. Chem. Phys.*, 5, 1053-1123, doi: 10.5194/acp-5-1053-2005, 2005.
- Kiendler-Scharr, A., Mensah, A. A., Frieze, E., Topping, D., Nemitz, E., Prevot, A. S. H., . . . Wu, H. C.: Ubiquity of organic nitrates from nighttime chemistry in the European submicron aerosol, *Geophys. Res. Lett.*, 43, 7735-7744, doi: 10.1002/2016gl069239, 2016.
- Koutrakis, P., Wolfson, J. M., and Spengler, J. D.: An improved method for measuring aerosol strong acidity: Results from a nine-month study in St Louis, Missouri and Kingston, Tennessee, *Atmos. Environ.* (1967), 22, 157-162, doi: 10.1016/0004-6981(88)90308-3, 1988.
- Krupa, S. V.: Effects of atmospheric ammonia (NH<sub>3</sub>) on terrestrial vegetation: a review, *Environ. Pollut.*, 124, 179-221, doi: 10.1016/s0269-7491(02)00434-7, 2003.
- Lelieveld, J., Evans, J. S., Fnais, M., Giannadaki, D., and Pozzer, A.: The contribution of outdoor air pollution sources to premature mortality on a global scale, *Nature*, 525, 367-371, doi: 10.1038/nature15371, 2015.
- Lim, S. S., Vos, T., Flaxman, A. D., Danaei, G., Shibuya, K., Adair-Rohani, H., . . . Ezzati, M.: A comparative risk assessment of burden of disease and injury attributable to 67 risk factors and risk factor clusters in 21 regions, 1990-2010: a systematic analysis for the Global Burden of Disease Study 2010, *Lancet*, 380, 2224-2260, doi: 10.1016/S0140-6736(12)61766-8, 2012.
- Lolkema, D. E., Noordijk, H., Stolk, A. P., Hoogerbrugge, R., van Zanten, M. C., and van Pul, W. A. J.: The Measuring Ammonia in Nature (MAN) network in the Netherlands, *Biogeosciences*, 12, 5133-5142, doi: 10.5194/bg-12-5133-2015, 2015.
- Longo, A. F., Feng, Y., Lai, B., Landing, W. M., Shelley, R. U., Nenes, A., . . . Ingall, E. D.: Influence of Atmospheric Processes on the Solubility and Composition of Iron in Saharan Dust, *Environ. Sci. Technol.*, 50, 6912-6920, doi: 10.1021/acs.est.6b02605, 2016.
- Meskhidze, N., Chameides, W. L., Nenes, A., and Chen, G.: Iron mobilization in mineral dust: Can anthropogenic SO<sub>2</sub> emissions affect ocean productivity?, *Geophys. Res. Lett.*, 30, 2085, doi: 10.1029/2003gl018035, 2003.

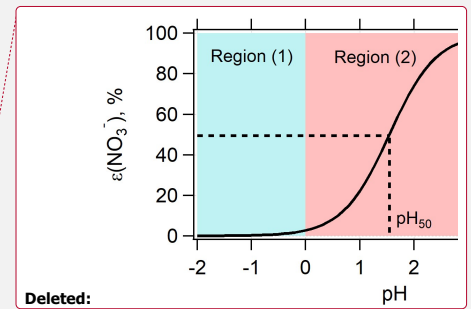
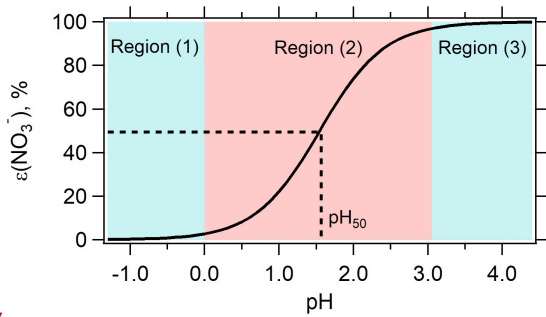
- Meskhidze, N., Chameides, W. L., and Nenes, A.: Dust and pollution: A recipe for enhanced ocean fertilization?, *J. Geophys. Res.*, 110, D03301, doi: 10.1029/2004jd005082, 2005.
- Nah, T., Guo, H., Sullivan, A. P., Chen, Y., Tanner, D. J., Nenes, A., . . . Weber, R. J.: Characterization of Aerosol Composition, Aerosol Acidity and Organic Acid Partitioning at an Agriculture-Intensive Rural Southeastern U.S. Site, *Atmos. Chem. Phys. Disc.*, 1-46, doi: 10.5194/acp-2018-373, 2018.
- Nenes, A., Krom, M. D., Mihalopoulos, N., Van Cappellen, P., Shi, Z., Bougiatioti, A., . . . Herut, B.: Atmospheric acidification of mineral aerosols: a source of bioavailable phosphorus for the oceans, *Atmos. Chem. Phys.*, 11, 6265-6272, doi: 10.5194/acp-11-6265-2011, 2011.
- 10 Paulot, F., and Jacob, D. J.: Hidden cost of U.S. agricultural exports: particulate matter from ammonia emissions, *Environ. Sci. Technol.*, 48, 903-908, doi: 10.1021/es4034793, 2014.
- Paulot, F., Fan, S., and Horowitz, L. W.: Contrasting seasonal responses of sulfate aerosols to declining SO<sub>2</sub> emissions in the Eastern U.S.: Implications for the efficacy of SO<sub>2</sub> emission controls, *Geophys. Res. Lett.*, 44, 455-464, doi: 10.1002/2016gl070695, 2017.
- 15 Perrin, A. E., Pusede, S. E., and Cohen, R. C.: An observational perspective on the atmospheric impacts of alkyl and multifunctional nitrates on ozone and secondary organic aerosol, *Chem. Rev.*, 113, 5848-5870, doi: 10.1021/cr300520x, 2013.
- Perrino, C., Catrambone, M., Di Menno Di Buccianico, A., and Allegrini, I.: Gaseous ammonia in the urban area of Rome, Italy and its relationship with traffic emissions, *Atmos. Environ.*, 36, 5385-5394, doi: 10.1016/s1352-2310(02)00469-7, 2002.
- 20 Pinder, R. W., Adams, P. J., and Pandis, S. N.: Ammonia Emission Controls as a Cost-Effective Strategy for Reducing Atmospheric Particulate Matter in the Eastern United States, *Environ. Sci. Technol.*, 41, 380-386, doi: 10.1021/es060379a, 2007.
- Pinder, R. W., Gilliland, A. B., and Dennis, R. L.: Environmental impact of atmospheric NH<sub>3</sub> emissions under present and future conditions in the eastern United States, *Geophys. Res. Lett.*, 35, L12808, doi: 10.1029/2008gl033732, 2008.
- 25 Pope, C. A., III, Burnett, R. T., Thurston, G. D., Thun, M. J., Calle, E. E., Krewski, D., and Godleski, J. J.: Cardiovascular mortality and long-term exposure to particulate air pollution: epidemiological evidence of general pathophysiological pathways of disease, *Circulation*, 109, 71-77, doi: 10.1161/01.CIR.0000108927.80044.7F, 2004.
- 30 Pozzer, A., Tsimpidi, A. P., Karydis, V. A., de Meij, A., and Lelieveld, J.: Impact of agricultural emission reductions on fine-particulate matter and public health, *Atmos. Chem. Phys.*, 17, 12813-12826, doi: 10.5194/acp-17-12813-2017, 2017.
- Pye, H. O. T., Zuend, A., Fry, J. L., Isaacman-VanWertz, G., Capps, S. L., Appel, K. W., . . . Goldstein, A. H.: Coupling of organic and inorganic aerosol systems and the effect on gas-particle partitioning in the southeastern US, *Atmos. Chem. Phys.*, 18, 357-370, doi: 10.5194/acp-18-357-2018, 2018.
- 35 Raizenne, M., Neas, L. M., Damokosh, A. I., Dockery, D. W., Spengler, J. D., Koutrakis, P., . . . Speizer, F. E.: Health effects of acid aerosols on North American children: pulmonary function, *Environ. Health Perspect.*, 104, 506-514, doi: 10.2307/3432991, 1996.
- 40 Rumsey, I. C., Cowen, K. A., Walker, J. T., Kelly, T. J., Hanft, E. A., Mishoe, K., . . . Otjes, R. P.: An assessment of the performance of the Monitor for AeRosols and GAses in ambient air (MARGA): a semi-continuous method for soluble compounds, *Atmos. Chem. Phys.*, 14, 5639-5658, doi: 10.5194/acp-14-5639-2014, 2014.



- Russell, A. R., Valin, L. C., and Cohen, R. C.: Trends in OMI NO<sub>2</sub> observations over the United States: effects of emission control technology and the economic recession, *Atmos. Chem. Phys.*, 12, 12197-12209, doi: 10.5194/acp-12-12197-2012, 2012.
- Sardar, S. B., Fine, P. M., and Sioutas, C.: Seasonal and spatial variability of the size-resolved chemical composition of particulate matter (PM<sub>10</sub>) in the Los Angeles Basin, *J. Geophys. Res.*, 110, D07S08, doi: 10.1029/2004jd004627, 2005.
- Schaap, M., Otjes, R. P., and Weijers, E. P.: Illustrating the benefit of using hourly monitoring data on secondary inorganic aerosol and its precursors for model evaluation, *Atmos. Chem. Phys.*, 11, 11041-11053, doi: 10.5194/acp-11-11041-2011, 2011.
- 10 Schlag, P., Kiendler-Scharr, A., Blom, M. J., Canonaco, F., Henzing, J. S., Moerman, M., . . . Holzinger, R.: Aerosol source apportionment from 1-year measurements at the CESAR tower in Cabauw, the Netherlands, *Atmos. Chem. Phys.*, 16, 8831-8847, doi: 10.5194/acp-16-8831-2016, 2016.
- Schlag, P., Rubach, F., Mentel, T. F., Reimer, D., Canonaco, F., Henzing, J. S., . . . Kiendler-Scharr, A.: Ambient and laboratory observations of organic ammonium salts in PM<sub>1</sub>, *Faraday Discuss.*, 200, 331-351, doi: 10.1039/c7fd00027h, 2017.
- 15 Schrader, F., and Brummer, C.: Land Use Specific Ammonia Deposition Velocities: a Review of Recent Studies (2004-2013), *Water Air Soil Pollut.*, 225, 2114, doi: 10.1007/s11270-014-2114-7, 2014.
- 20 Shah, V., Jaeglé, L., Thornton, J. A., Lopez-Hilfiker, F. D., Lee, B. H., Schroder, J. C., . . . Brown, S. S.: Chemical feedbacks weaken the wintertime response of particulate sulfate and nitrate to emissions reductions over the eastern United States, *Proc. Natl. Acad. Sci. U.S.A.*, doi: 10.1073/pnas.1803295115, 2018.
- Skjoth, C. A., and Geels, C.: The effect of climate and climate change on ammonia emissions in Europe, *Atmos. Chem. Phys.*, 13, 117-128, doi: 10.5194/acp-13-117-2013, 2013.
- 25 Song, S., Gao, M., Xu, W., Shao, J., Shi, G., Wang, S., . . . McElroy, M. B.: Fine-particle pH for Beijing winter haze as inferred from different thermodynamic equilibrium models, *Atmos. Chem. Phys.*, 18, 7423-7438, doi: 10.5194/acp-18-7423-2018, 2018.
- Stockdale, A., Krom, M. D., Mortimer, R. J., Benning, L. G., Carslaw, K. S., Herbert, R. J., . . . Nenes, A.: Understanding the nature of atmospheric acid processing of mineral dusts in supplying bioavailable phosphorus to the oceans, *Proc. Natl. Acad. Sci. U.S.A.*, 113, 14639-14644, doi: 10.1073/pnas.1608136113, 2016.
- 30 Surratt, J. D., Chan, A. W., Eddingsaas, N. C., Chan, M., Loza, C. L., Kwan, A. J., . . . Seinfeld, J. H.: Reactive intermediates revealed in secondary organic aerosol formation from isoprene, *Proc. Natl. Acad. Sci. U.S.A.*, 107, 6640-6645, doi: 10.1073/pnas.0911114107, 2010.
- 35 Thurston, G. D., Ito, K., Hayes, C. G., Bates, D. V., and Lippmann, M.: Respiratory hospital admissions and summertime haze air pollution in Toronto, Ontario: consideration of the role of acid aerosols, *Environ. Res.*, 65, 271-290, doi: 10.1006/enrs.1994.1037, 1994.
- Tsimpidi, A. P., Karydis, V. A., and Pandis, S. N.: Response of Inorganic Fine Particulate Matter to Emission Changes of Sulfur Dioxide and Ammonia: The Eastern United States as a Case Study, *J Air Waste Manag. Assoc.*, 57, 1489-1498, doi: 10.3155/1047-3289.57.12.1489, 2007.
- 40 Vasilakos, P., Russell, A., Weber, R., and Nenes, A.: Understanding nitrate formation in a world with less sulfate, *Atmos. Chem. Phys. Disc.*, 1-27, doi: 10.5194/acp-2018-406, 2018.

- Wang, G., Zhang, R., Gomez, M. E., Yang, L., Levy Zamora, M., Hu, M., . . . Molina, M. J.: Persistent sulfate formation from London Fog to Chinese haze, *Proc. Natl. Acad. Sci. U.S.A.*, 113, 13630-13635, doi: 10.1073/pnas.1616540113, 2016.
- Wang, S., Xing, J., Jang, C., Zhu, Y., Fu, J. S., and Hao, J.: Impact assessment of ammonia emissions on inorganic aerosols in East China using response surface modeling technique, *Environ. Sci. Technol.*, 45, 9293-9300, doi: 10.1021/es2022347, 2011.
- Warner, J. X., Wei, Z., Strow, L. L., Dickerson, R. R., and Nowak, J. B.: The global tropospheric ammonia distribution as seen in the 13-year AIRS measurement record, *Atmos. Chem. Phys.*, 16, 5467-5479, doi: 10.5194/acp-16-5467-2016, 2016.
- 10 Warner, J. X., Dickerson, R. R., Wei, Z., Strow, L. L., Wang, Y., and Liang, Q.: Increased atmospheric ammonia over the world's major agricultural areas detected from space, *Geophys. Res. Lett.*, doi: 10.1002/2016gl072305, 2017.
- Weber, R. J., Guo, H., Russell, A. G., and Nenes, A.: High aerosol acidity despite declining atmospheric sulfate concentrations over the past 15 years, *Nat. Geosci.*, 9, 282-285, doi: 10.1038/ngeo2665, 2016.
- 15 Wells, M., Choularton, T. W., and Bower, K. N.: A modelling study of the interaction of ammonia with cloud, *Atmos. Environ.*, 32, 359-363, doi: 10.1016/s1352-2310(97)00199-4, 1998.
- Xu, L., Suresh, S., Guo, H., Weber, R. J., and Ng, N. L.: Aerosol characterization over the southeastern United States using high-resolution aerosol mass spectrometry: spatial and seasonal variation of aerosol composition and sources with a focus on organic nitrates, *Atmos. Chem. Phys.*, 15, 7307-7336, doi: 10.5194/acp-15-7307-2015, 2015.
- Yamamoto, N., Kabeya, N., Onodera, M., Takahashi, S., Komori, Y., Nakazuka, E., and Shirai, T.: Seasonal variation of atmospheric ammonia and particulate ammonium concentrations in the urban atmosphere of yokohama over a 5-year period, *Atmos. Environ.* (1967), 22, 2621-2623, doi: 10.1016/0004-6981(88)90498-2, 1988.
- 25 Young, A. H., Keene, W. C., Pszenny, A. A. P., Sander, R., Thornton, J. A., Riedel, T. P., and Maben, J. R.: Phase partitioning of soluble trace gases with size-resolved aerosols in near-surface continental air over northern Colorado, USA, during winter, *J. Geophys. Res.*, 118, 9414-9427, doi: 10.1002/jgrd.50655, 2013.
- 30 Zhang, L., Chen, Y., Zhao, Y., Henze, D. K., Zhu, L., Song, Y., . . . Huang, B.: Agricultural ammonia emissions in China: reconciling bottom-up and top-down estimates, *Atmos. Chem. Phys.*, 18, 339-355, doi: 10.5194/acp-18-339-2018, 2018.
- Zhang, Q., Jimenez, J. L., Canagaratna, M. R., Allan, J. D., Coe, H., Ulbrich, I., . . . Worsnop, D. R.: Ubiquity and dominance of oxygenated species in organic aerosols in anthropogenically-influenced Northern Hemisphere midlatitudes, *Geophys. Res. Lett.*, 34, L13801, doi: 10.1029/2007gl029979, 2007.
- 35 Zhu, S., Sartelet, K., Zhang, Y., and Nenes, A.: Three-dimensional modeling of the mixing state of particles over Greater Paris, *J. Geophys. Res.*, 121, 5930-5947, doi: 10.1002/2015jd024241, 2016.
- 40 Zhu, S., Horne, J. R., Montoya-Aguilera, J., Hinks, M. L., Nizkorodov, S. A., and Dabdub, D.: Modeling reactive ammonia uptake by secondary organic aerosol in CMAQ: application to the continental US, *Atmos. Chem. Phys.*, 18, 3641-3657, doi: 10.5194/acp-18-3641-2018, 2018.

45



Deleted:

**Figure 1.** Predicted particle phase fraction of total nitrate,  $\varepsilon(\text{NO}_3^-)$ , versus pH for one-year

5 average condition in Cabauw based on Eq. (4). The blue-color zone denotes where  $\text{HNO}_3\text{-NO}_3^-$  (nitric acid-nitrate) partitioning is not affected by changes in pH, while the red-color zone shows the region where adjusting pH will change  $\text{HNO}_3\text{-NO}_3^-$  partitioning, hence  $\text{NO}_3^-$  concentration. Greatest sensitivity  $\text{NO}_3^-$  occurs at  $\varepsilon(\text{NO}_3^-) = 50\%$ , corresponding to  $\text{pH}_{50}$ .

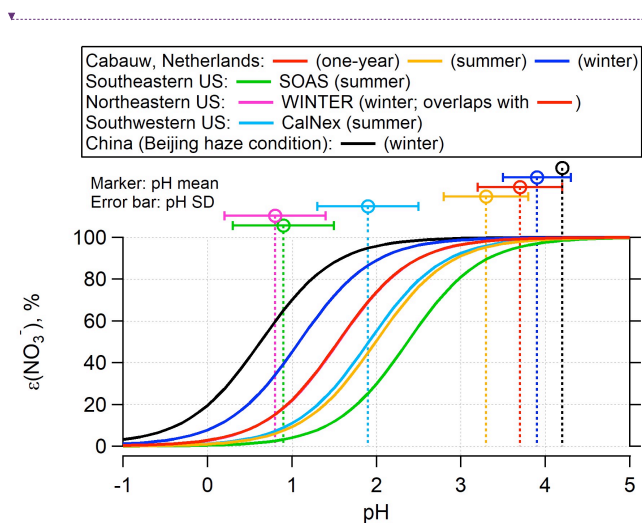
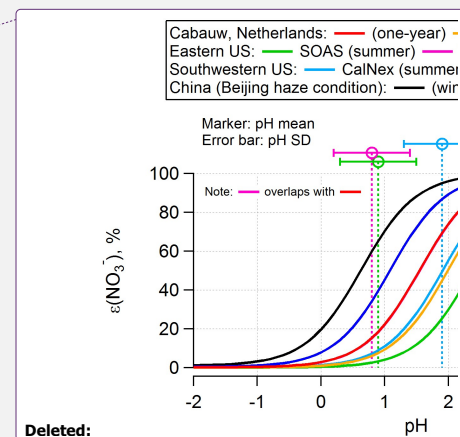


**Figure 2.**  $\epsilon(\text{NO}_3^-)$  versus pH for various field studies based on the average temperature, liquid water, and activity coefficients for each study, according to Eq. (4). The WINTER study curve overlaps completely with the Cabauw one-year average curve in red color. The input can be found in Table S1. Vertical lines are the study average ambient fine particle pH calculated with ISORROPIA-II and error bars show the variability in pH as one standard deviation. S-curves and ambient pH for each site or season can be matched by color. For a more direct comparison between seasons at a specific region, supplemental Fig. S5 shows separate curves and ambient pH plots.



Deleted: S4

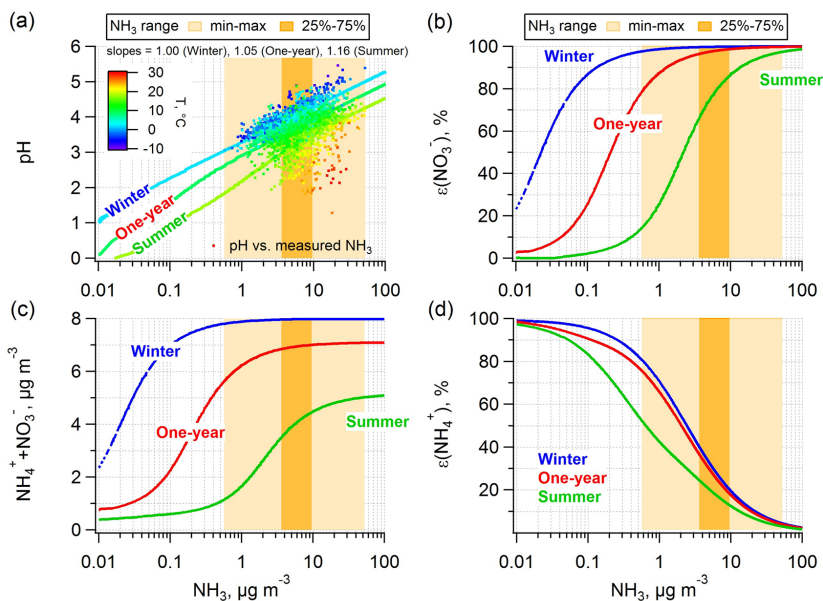


**Figure 3.** Prediction of (a) particle pH, (b) particle phase fractions of total nitrate,  $\varepsilon(\text{NO}_3^-)$ , (c) ammonium and nitrate mass concentration, (d) particle phase fractions of total ammonium,  $\varepsilon(\text{NH}_4^+)$  for a wide range of ammonia. The simulations are based on the one-year (July 2012-5 June 2013), summer (June-Aug 2012), and winter (Dec 2012-Feb 2013) average conditions at the Cabauw site with  $\text{NH}_x$  ( $\text{NH}_4^+ + \text{NH}_3$ ) left as a free variable. The measured  $\text{NH}_3$  ranges for the one-year span are also shown as the lighter (min-max) and darker (25%-75% percentiles) orange-color zones. Plot (a) also includes the predicted pH versus measured  $\text{NH}_3$  data for the entire study and colored by ambient temperature.

Deleted: 1-hr average

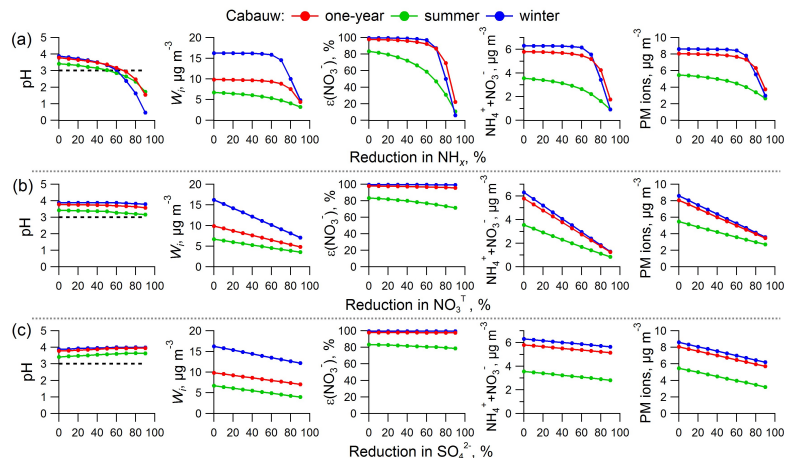


**Figure 4.** ISORROPIA-predicted PM<sub>2.5</sub> pH (1<sup>st</sup> column), liquid water content ( $W_t$ , 2<sup>nd</sup> column),  $\epsilon(\text{NO}_3^-)$  (3<sup>rd</sup> column), ammonium and nitrate (4<sup>th</sup> column), and aerosol inorganic mass

Deleted: ,

concentrations (5<sup>th</sup> column) as a function of changes in  $\text{NH}_x$  ( $\text{NH}_4^+ + \text{NH}_3$ , 1<sup>st</sup> row),  $\text{NO}_3^T$  ( $\text{NO}_3^- + \text{HNO}_3$ , 2<sup>nd</sup> row), and  $\text{SO}_4^{2-}$  (3<sup>rd</sup> row). Simulations are based on average conditions of one-year, summer, and winter observational data in Cabauw, the Netherlands, and changing only  $\text{NH}_x$ ,  $\text{NO}_3^T$  and  $\text{SO}_4^{2-}$  from the average conditions. The black dash lines in the pH figures identifies the critical pH value of 3.

Deleted: refer

Deleted: to a pH

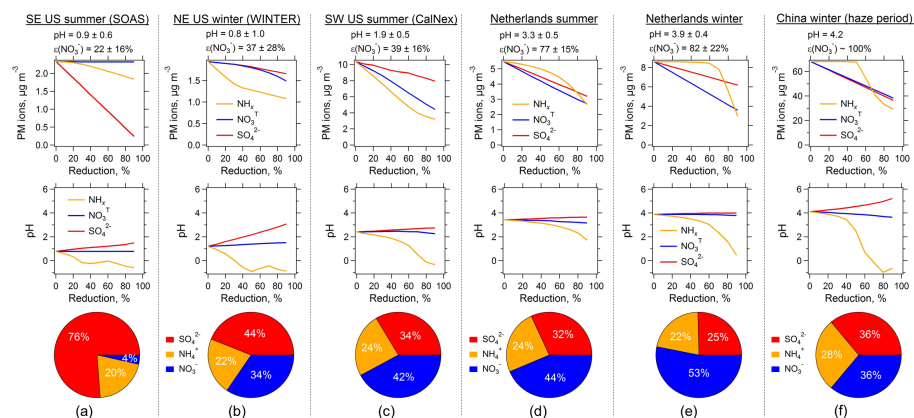


**Figure 5.** Response of predicted  $PM_{2.5}$  inorganic mass concentration (1<sup>st</sup> row) and pH (2<sup>nd</sup> row) to reduced levels of  $NH_x$  ( $NH_3 + NH_4^+$ ),  $NO_3^T$  ( $HNO_3 + NO_3^-$ ), and  $SO_4^{2-}$  for several studies including: (a) the southeastern US summer at a rural ground site in Centreville, AL (SOAS study), (b) the northeastern US during winter (WINTER aircraft study), (c) the southwestern US summer at an urban site in Pasadena, CA (CalNex study), (d) & (e) the Netherlands summer and winter conditions at an rural site in Cabauw from this study, and (f) polluted winter conditions (haze) in Beijing, China. For each case, the average fine ambient particle pH and  $\epsilon(NO_3^-)$ , prior to the reductions, are shown above the figures, with the columns ordered with increasing ambient particle pH from left to right.  $PM_{2.5}$  mass fractions of  $NH_4^+$ - $SO_4^{2-}$ - $NO_3^-$  based on study averages are shown as pie graphs along the bottom.

## Effectiveness of Ammonia Reduction on Control of Fine Particle Nitrate

Hongyu Guo<sup>1</sup>, Rene Otjes<sup>2</sup>, Patrick Schlag<sup>3,4,5</sup>, Astrid Kiendler-Scharr<sup>4</sup>, Athanasios Nenes<sup>1,6,7,8</sup>, Rodney J. Weber<sup>1</sup>

<sup>1</sup> School of Earth and Atmospheric Sciences, Georgia Institute of Technology, Atlanta, GA 30332, USA

<sup>2</sup> Energy Research Centre of the Netherlands (ECN), Petten, [the](#) Netherlands

<sup>3</sup> Utrecht University, Utrecht, [the](#) Netherlands

<sup>4</sup> Institute for Energy and Climate Research (IEK-8): Troposphere, Forschungszentrum Jülich, Jülich, Germany

<sup>5</sup> Now at University of Sao Paulo, SP, Brazil

<sup>6</sup> School of Chemical and Biomolecular Engineering, Georgia Institute of Technology, Atlanta, GA 30332, USA

<sup>7</sup> Institute for Chemical Engineering Sciences, Foundation for Research and Technology – Hellas, Patras, GR-26504, Greece

<sup>8</sup> Institute for Environmental Research and Sustainable Development, National Observatory of Athens, P. Penteli, Athens, GR-15236, Greece

\* To whom correspondence should be addressed: [rweber@eas.gatech.edu](mailto:rweber@eas.gatech.edu)

### Contents of this file

**Figures S1-S9**

**Table S1**

**Formatted:** Space After: 0 pt

**Deleted:** 8



# 1. Diurnal profiles of T, RH and pH in Cabauw, Netherlands

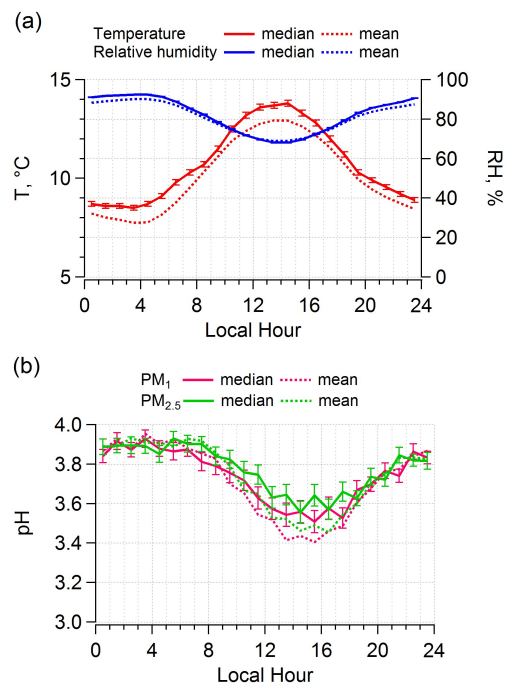


**Fig. S1.** For the one-year observation at CESAR tower, diurnal profiles of (a) measured T, RH, (b) predicted PM<sub>1</sub> and PM<sub>2.5</sub> pH. Mean hourly medians and means are shown and standard errors are plotted as error bars.

## 2. The thermodynamic model and comparison of predicted and measured gas-particle partitioning in Cabauw, Netherlands

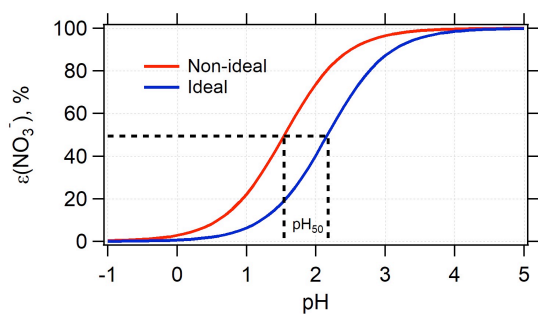


**Fig. S2.** Predicted particle phase fraction of total nitrate,  $\varepsilon(\text{NO}_3^-)$ , versus pH for one-year average condition in Cabauw based on Eq. (4) in the main text. The red and blue lines are based on  $\gamma_{\text{NO}_3^-}\gamma_{\text{H}^+} = 0.24$  (extracted from ISORROPIA-II) and 1 (ideal solution), respectively.

Formatted: Heading 3, Line spacing: single

### 3. The thermodynamic model and comparison of predicted and measured gas-particle partitioning in Cabauw, Netherlands

pH of PM<sub>1</sub> or PM<sub>2.5</sub> was determined from running the Windows stand-alone executable version of ISORROPIA-II ([http://isorro피아.eas.gatech.edu/index.php?title=Main\\_Page](http://isorro피아.eas.gatech.edu/index.php?title=Main_Page)) in forward and metastable modes. The model has been proven to accurately predict gas-aerosol partitioning of inorganic species in many studies (Fountoukis and Nenes, 2007; Guo et al., 2016; Guo et al., 2017a; Liu et al., 2017), including particle liquid water (Guo et al., 2015; Bougiatioti et al., 2016). ISORROPIA-II has been used to predict particle pH in several studies (Guo et al., 2015; Hennigan et al., 2015; Guo et al., 2016; Guo et al., 2017a; Liu et al., 2017). pH is a logarithmic scale of hydronium ion activity in an aqueous solution,

$$\text{pH} = -\log_{10} \gamma_{\text{H}^+} H_{\text{aq}}^+ = -\log_{10} \frac{1000 \gamma_{\text{H}^+} H_{\text{air}}^+}{W_i + W_o} \cong -\log_{10} \frac{1000 \gamma_{\text{H}^+} H_{\text{air}}^+}{W_i} \quad (1)$$

where  $\gamma_{\text{H}^+}$  is the hydronium ion activity coefficient.  $\gamma_{\text{H}^+}$  is assumed = 1, however, ISORROPIA-II calculates the activity coefficients of ionic pairs, such as  $\text{H}^+ \text{-NO}_3^-$ , so the nonideality effect of  $\text{H}^+$  is considered),  $H_{\text{aq}}^+$  (mol L<sup>-1</sup>) is the hydronium ion concentration in particle liquid water,  $H_{\text{air}}^+$  (μg m<sup>-3</sup>) is the hydronium ion concentration per volume of air, and  $W_i$ ,  $W_o$  (μg m<sup>-3</sup>) are particle water concentrations associated with inorganic and organic species, respectively. pH predicted solely with  $W_i$  is fairly accurate; pH was 0.15-0.23 units systematically lower than and highly correlated to ( $r^2 = 0.97$ ) pH predicted with total particle water ( $W_i + W_o$ ) in the southeastern US, where  $W_o$  was on average 35% of total particle water (Guo et al., 2015). In most other location, including this study, a smaller contribution from  $W_o$  is expected based on the smaller organic aerosol mass fraction, 29%, (Schlag et al., 2016) compared to the southeastern US, ~60% (Xu et al., 2015). For this study of Cabauw, we only use  $W_i$  for the following pH calculations.

As in past studies (Guo et al., 2015; Guo et al., 2016; Guo et al., 2017a), predicted pH was assessed by comparing measured and model-predicted gas-aerosol partitioning of semi-volatile species, such as  $\text{NH}_3$ - $\text{NH}_4^+$ ,  $\text{HNO}_3$ - $\text{NO}_3^-$ ,  $\text{HCl}$ - $\text{Cl}^-$ , when not completely in the gas or aerosol phase. An accurate pH prediction is important in this study, as the nitrate gas-particle partitioning is pH dependent (Guo et al., 2016).

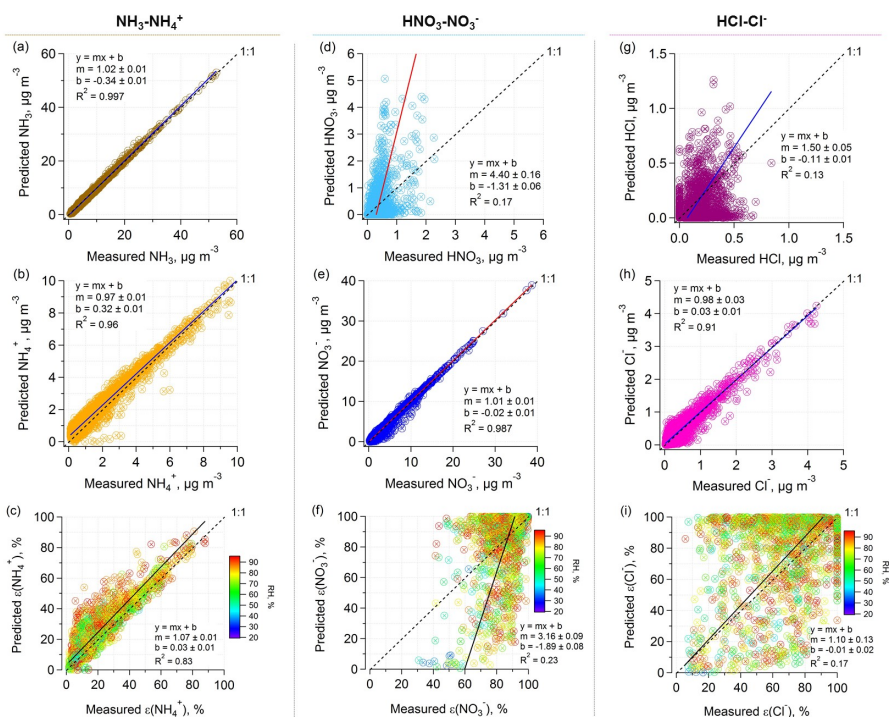


**Fig. S3.** Comparisons of predicted and measured  $\text{NH}_3$ ,  $\text{NH}_4^+$ , and  $\epsilon(\text{NH}_4^+)$  (a, b, c),  $\text{HNO}_3$ ,  $\text{NO}_3^-$ , and  $\epsilon(\text{NO}_3^-)$  (d, e, f), and  $\text{HCl}$ ,  $\text{Cl}^-$ , and  $\epsilon(\text{Cl}^-)$  (g, h, i) for data from the one-year observational study at CESAR ground site. Gas- and particle-phase ( $\text{PM}_{2.5}$ ) data are all from MARGA. Low concentrations within  $2 \times \text{LOD}$  are excluded in plotting particle phase fractions due to high uncertainties. Orthogonal distance regression (ODR) fits are shown and uncertainties in the fits are one standard deviation (SD). Less agreement for gas phase  $\text{HNO}_3$  and  $\text{HCl}$  are thought to be due to significantly lower concentrations than the particle phase component ( $\text{NO}_3^-$ ,  $\text{Cl}^-$ , respectively). Bias in these gases can be possible if some particles are captured in the denuder, given that the ion chromatographic detection system can not distinguish between gas and particle phases ( $\text{NO}_3^-$  and  $\text{Cl}^-$  is measured for both).

Deleted: S2

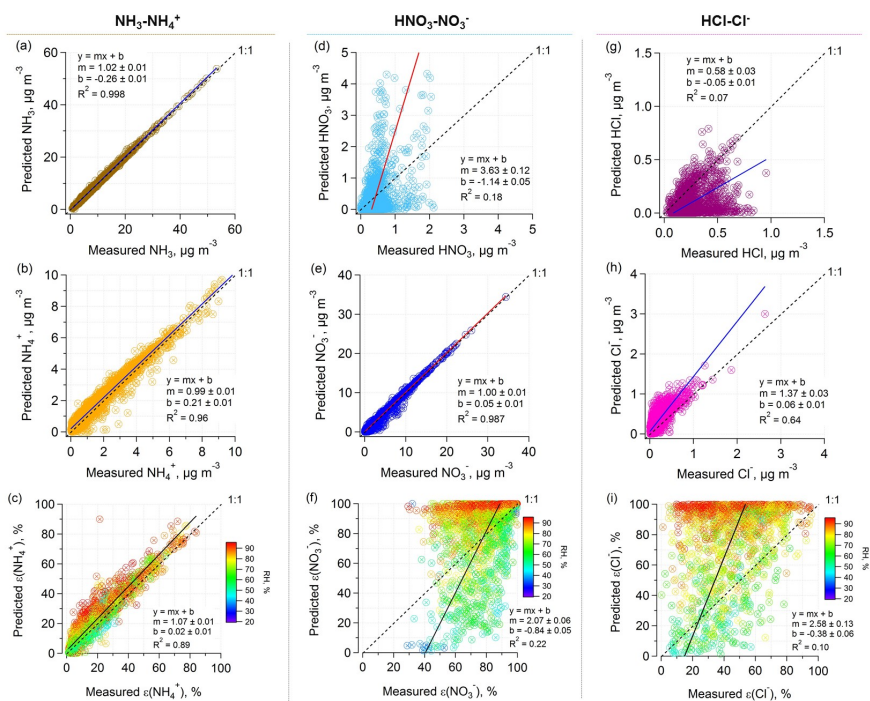
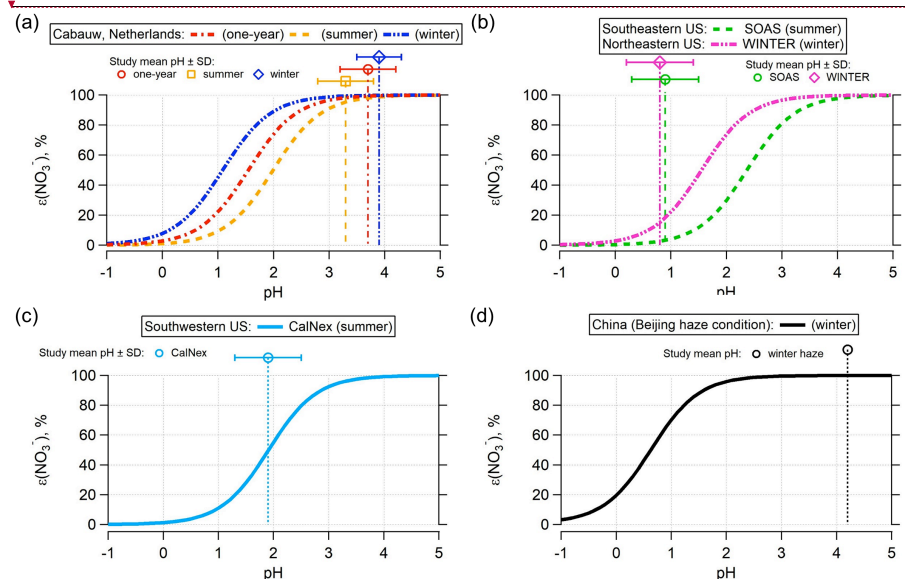


Fig. S4. A similar plot as Fig. S3. MARGA  $\text{PM}_{10}$  data was used in the model input instead of  $\text{PM}_{2.5}$ .

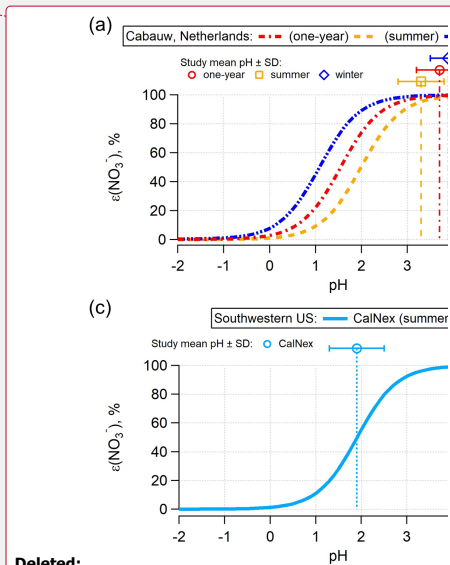
Deleted: S3

Deleted: S2

#### 4. Analytically predicted nitrate partitioning versus pH for various field studies



**Fig. S5.**  $\epsilon(\text{NO}_3^-)$  versus pH for the listed field studies. The S curves are calculated based on the average temperature, liquid water, and activity coefficients for each study, according to Eq. (4). The input can be found in Table S1. Vertical lines are the study average ambient fine particle pH calculated with ISORROPIA-II and error bars show the variability in pH as one standard deviation. This figure is reproduced from Figure 2 in the main text, to directly show the seasonal variations at a specific region.



Deleted:

Deleted: S4

## 5. Comparison of ISORROPIA-II predicted and analytically predicted pH

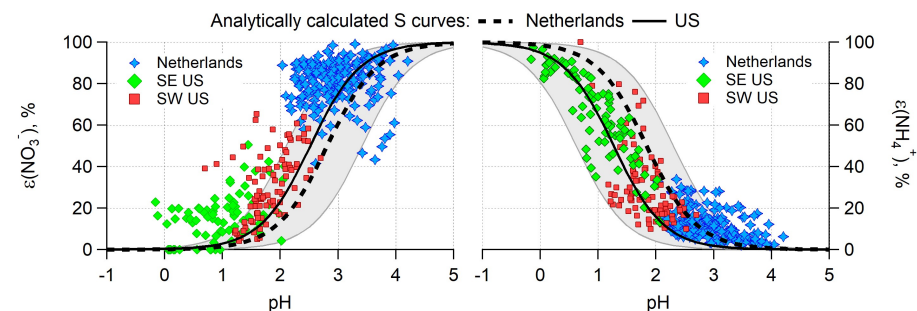
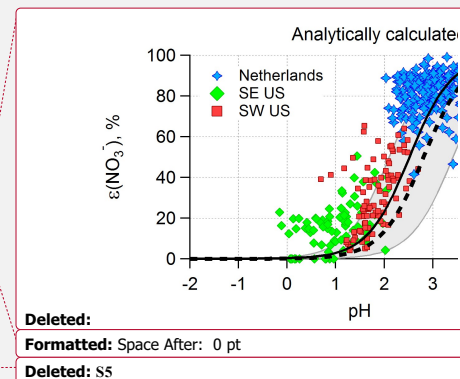


**Fig. S6.** Analytically calculated S curves of  $\epsilon(\text{NO}_3^-)$  and  $\epsilon(\text{NH}_4^+)$  (shown as lines), and observed ambient  $\epsilon(\text{NO}_3^-)$  and  $\epsilon(\text{NH}_4^+)$  plotted with ISORROPIA-predicted pH for SOAS (SE US), CalNex (SW US), and this study at Cabauw (Netherlands) (shown as data points).  $\epsilon(\text{NO}_3^-)$  and  $\epsilon(\text{NH}_4^+)$  are the particle fraction of gas plus particle for nitrate and ammonium, respectively. The analytical calculations are based on simple thermodynamic equations that can be found in the main text, Eq. (4) for  $\epsilon(\text{NO}_3^-)$  or in Guo et al. (2017a) and are independent of ISORROPIA-II calculations. Plotted data are for a relatively narrow range in  $W_i$  (1 to 4  $\mu\text{g m}^{-3}$ ) and T (15 to 25 °C) for comparison with the analytical calculation based on  $W_i = 2.5 \mu\text{g m}^{-3}$  and T = 20 °C. For the analytical calculations (the black solid and dashed S curves), ISORROPIA-II predicted activity coefficients are applied. For the selected water and temperature ranges,  $\gamma_{\text{H}^+}\gamma_{\text{NO}_3^-}$  is  $0.17 \pm 0.10$  for Cabauw,  $0.086 \pm 0.060$  for SE US, and  $0.087 \pm 0.027$  for SW US and  $\gamma_{\text{H}^+}/\gamma_{\text{NH}_4^+}$  is  $5.93 \pm 6.48$  for Cabauw,  $1.17 \pm 0.12$  for SE US, and  $1.90 \pm 0.12$  for SW US. Since the activity coefficients for the US studies are similar, they were averaged to produce one curve for SE US and SW US. Averaged  $\gamma_{\text{H}^+}/\gamma_{\text{NH}_4^+} = 1.6$  and  $\gamma_{\text{H}^+}\gamma_{\text{NO}_3^-} = 0.087$ . Some of the data scatter can be attributed to variations in liquid water, temperature, and activity coefficients. These effects are illustrated by the light gray shaded regions, which were plotted with different  $W_i$ , T, and  $\gamma_{\text{H}^+}\gamma_{\text{NO}_3^-}$  or  $\gamma_{\text{H}^+}/\gamma_{\text{NH}_4^+}$ . For example, the upper line for  $\epsilon(\text{NO}_3^-)$  is calculated using  $W_i = 4 \mu\text{g m}^{-3}$ , T = 15 °C, and  $\gamma_{\text{H}^+}\gamma_{\text{NO}_3^-} = 0.087$ , while the lower line is calculated using  $W_i = 1 \mu\text{g m}^{-3}$ , T = 25 °C, and  $\gamma_{\text{H}^+}\gamma_{\text{NO}_3^-} = 0.17$ . For  $\epsilon(\text{NH}_4^+)$ , the upper line for is calculated using  $W_i = 4 \mu\text{g m}^{-3}$ , T = 15 °C, and  $\gamma_{\text{H}^+}/\gamma_{\text{NH}_4^+} = 5.93$ , while the lower line is calculated using  $W_i = 1 \mu\text{g m}^{-3}$ , T = 25 °C, and  $\gamma_{\text{H}^+}/\gamma_{\text{NH}_4^+} = 1.6$ .



## 6. Temperature dependencies of $\text{NH}_3$ and $\text{HNO}_3$ gas-particle partitioning

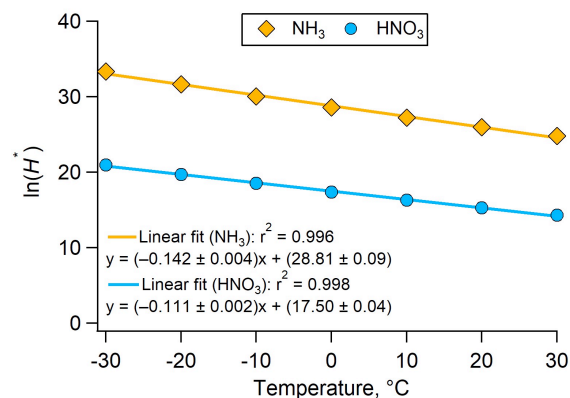


**Fig. S7.** Molality-based equilibrium constants ( $H^*$ ) of  $\text{NH}_3$ - $\text{NH}_4^+$  and  $\text{HNO}_3$ - $\text{NO}_3^-$  partitioning as a function of temperature.  $H_{\text{NH}_3}^*$  ( $\text{atm}^{-1}$ ) is for  $\text{NH}_{3(g)} + \text{H}^+ \leftrightarrow \text{NH}_4^+$  and  $H_{\text{HNO}_3}^*$  ( $\text{mole}^2 \text{kg}^{-2} \text{atm}^{-1}$ ) is for  $\text{HNO}_{3(g)} \leftrightarrow \text{NO}_3^- + \text{H}^+$ . The  $H_{\text{NH}_3}^*$  and  $H_{\text{HNO}_3}^*$  are calculated based on Clegg et al. (1998) and Clegg and Brimblecombe (1990), respectively, with a typo correction for the equation of  $H_{\text{NH}_3}^*$ . The correction and some instructions to calculate  $H^*$  can be found in the supplemental material of Guo et al. (2017a).  $H_{\text{NH}_3}^*$  decreases faster with increasing temperature compared to  $H_{\text{HNO}_3}^*$  (slope: -0.142 vs. -0.111), resulting in a net increase in particle  $\text{H}^+$ .

Deleted: S6



## 7. Particle nitrate and total inorganic mass reduction simulations at less sulfate or more nonvolatile cations condition

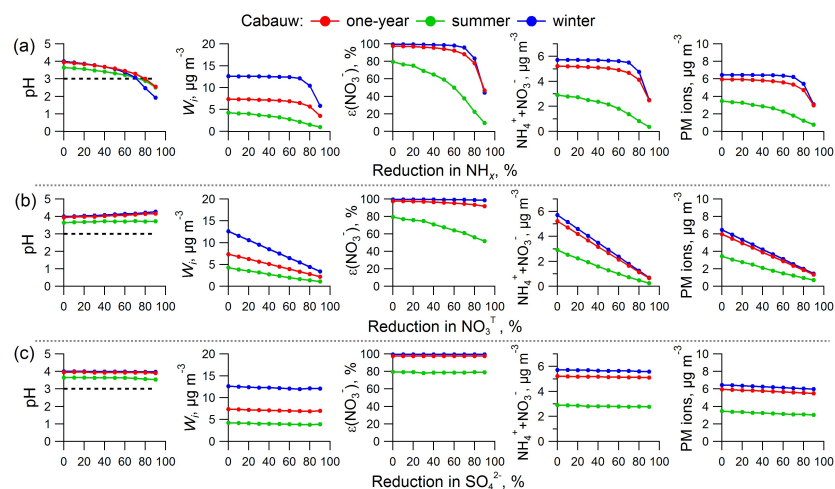


**Fig. S8.** Similar graph to Figure 4 in the main text, but for simulations with sulfate at 20% of the observed sulfate level while keeping all other inputs unchanged. The prediction of particle pH (1<sup>st</sup> column), liquid water content ( $W_l$ , 2<sup>nd</sup> column), nitrate particle-phase fraction ( $\epsilon(\text{NO}_3^-)$ , 3<sup>rd</sup> column), ammonium and nitrate (4<sup>th</sup> column), and total aerosol inorganic mass concentrations (5<sup>th</sup> column) for reduction of  $\text{NH}_4^+$  ( $\text{NH}_4^+ + \text{NH}_3$ , 1<sup>st</sup> row),  $\text{NO}_3^-$  ( $\text{NO}_3^- + \text{HNO}_3$ , 2<sup>nd</sup> row), and  $\text{SO}_4^{2-}$  (3<sup>rd</sup> row) with the base case the average conditions of one-year (July 2012-June 2013), summer (June-Aug 2012), and winter (Dec 2012-Feb 2013) observational data in Cabauw, Netherlands. [The black dash lines in the pH figures identifies the critical pH value of 3.](#)

Deleted: S7

Deleted: The black dash lines in pH figures refer to a pH value of 3.

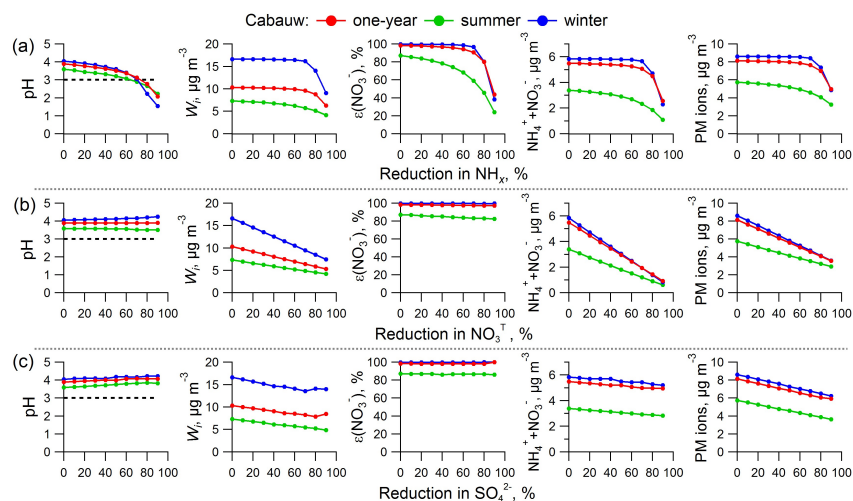


**Fig. S9.** A similar graph to Figure 4 in the main text and Fig. S8 in the supplement. The above figure shows results with five times of the observed nonvolatile cation levels, while keeping other inputs unchanged. The black dash lines in the pH figures identifies the critical pH value of 3.

Deleted: S8

Deleted: S4

Deleted: The black dash lines in pH figures refer to a pH value of 3.

**8. Summary of thermodynamic modeling inputs and outputs based on the observational averages in Cabauw, Netherlands, and previously published observational averages at several other sites.**

**Table. S1.** Study average aerosol composition and meteorological conditions for various sites. Various concentrations, RH, and T are based on field measurements, unless noted specifically.

(Region) Country	SE US	NE US	SW US	Netherlands			China
Site location	Centreville, AL	Hampton, VA	Pasadena, CA	Cabauw			Beijing
Campaign	SOAS	WINTER	CalNex	EU-FP7-ACTRIS (Q-ACSM Network)			\
Sampling type	Ground	Aircraft	Ground	Ground			Ground
PM cut size	PM <sub>1</sub> &PM <sub>2.5</sub> <sup>a</sup>	PM <sub>1</sub>	PM <sub>1</sub> <sup>c</sup>	PM <sub>2.5</sub>			PM <sub>1</sub>
Year	2013	2015	2010	2012-2013			2013
Season	Summer	Winter	(Early) Summer	One-year	Summer	Winter	Winter
Na <sup>+</sup> , µg m <sup>-3</sup>	0.03	0	0	0.14	0.17	0.15	0
SO <sub>4</sub> <sup>2-</sup> , µg m <sup>-3</sup>	1.73	1.02	2.86	2.20	1.86	2.51	26
NH <sub>4</sub> <sup>+</sup> +NH <sub>3</sub> , µg m <sup>-3</sup>	0.78	0.50	3.44	9.63	11.44	6.73	32.8
NO <sub>3</sub> <sup>-</sup> +HNO <sub>3</sub> , µg m <sup>-3</sup>	0.45	2.21	10.22	4.87	3.48	5.50	26
Cl <sup>-</sup> +HCl, µg m <sup>-3</sup>	0.02	0	0	0.53	0.44	0.54	1.7
Ca <sup>2+</sup> , µg m <sup>-3</sup>	0	0	0	0.01	0.02	0.001	0
K <sup>+</sup> , µg m <sup>-3</sup>	0	0	0	0.004	0.01	0.002	0
Mg <sup>2+</sup> , µg m <sup>-3</sup>	0	0	0	0.03	0.01	0.04	0
RH, %	74	58	79	78	78	85	56
T, °C	24.7	-0.4	18.3	9.0	17.8	2.4	0.9
NH <sub>4</sub> <sup>+</sup> , µg m <sup>-3</sup>	0.46	0.50	2.06	1.90	1.51	2.13	20
NH <sub>3</sub> , µg m <sup>-3</sup>	0.39	0.10 <sup>b</sup>	1.37	7.73	9.94	4.60	12.8
ε(NH <sub>4</sub> <sup>+</sup> ), %	59	91 <sup>b</sup>	56	19	14	27	60
NO <sub>3</sub> <sup>-</sup> , µg m <sup>-3</sup>	0.08	0.80	3.58	4.53	3.08	5.28	26
HNO <sub>3</sub> , µg m <sup>-3</sup>	0.36	1.41	6.65	0.35	0.40	0.22	\
ε(NO <sub>3</sub> <sup>-</sup> ), %	22	39	39	88	84	91	\
HCl, µg m <sup>-3</sup>	\	\	\	0.13	0.16	0.03	\
Cl <sup>-</sup> , µg m <sup>-3</sup>	0.02	0	0	0.40	0.28	0.51	1.7
ε(Cl <sup>-</sup> ), %	\	\	\	66	52	89	\
γ <sub>NO<sub>3</sub></sub> -γ <sub>H<sup>+</sup></sub>	0.08	0.06	0.14	0.24	0.20	0.24	0.11 <sup>d</sup>
Liquid water, µg m <sup>-3</sup>	5.1	2.0	13.9	21.7	15.7	31.4	35.1 <sup>d</sup>
ΔpH/Δ(log <sub>10</sub> NH <sub>3</sub> )	1.01	1.03	1.07	1.05	1.16	1.00	1.00 <sup>d</sup>
pH	0.9 ± 0.6	0.8 ± 1.0	1.9 ± 0.5	3.7 ± 0.5	3.3 ± 0.5	3.9 ± 0.4	4.2 <sup>d</sup>
Reference	(Guo et al., 2015)	(Guo et al., 2016)	(Guo et al., 2017a)	This study			(Wang et al., 2016)

<sup>a</sup> PM<sub>2.5</sub> was sampled in the 1<sup>st</sup> half and PM<sub>1</sub> sampled in the 2<sup>nd</sup> half of the study; various parameters were similar in both cases, crustal components were higher in PM<sub>2.5</sub>, but generally low so differences had minor effects, e.g., PM<sub>2.5</sub> Na<sup>+</sup> was 0.06 ± 0.09 µg m<sup>-3</sup> and PM<sub>1</sub> Na<sup>+</sup> was 0.01 ± 0.01 µg m<sup>-3</sup>; <sup>b</sup> Prediction based on iteration; <sup>c</sup> PM<sub>2.5</sub> data was only available for the last week, so here we focus on PM<sub>1</sub> collected throughout the campaign; <sup>d</sup> The model results are from another publication, Guo et al. (2017b).

ISOROP/A-II input

Input related parameters

ISOROP/A-II output

## References

- Bougiatioti, A., Nikolaou, P., Stavroulas, I., Kouvarakis, G., Weber, R., Nenes, A., Kanakidou, M., and Mihalopoulos, N.: Particle water and pH in the Eastern Mediterranean: Sources variability and implications for nutrients availability, *Atmos. Chem. Phys.*, 16, 4579-4591, doi: 10.5194/acp-16-4579-2016, 2016.
- Clegg, S. L., and Brimblecombe, P.: Equilibrium partial pressures and mean activity and osmotic coefficients of 0-100% nitric acid as a function of temperature, *Journal of Physical Chemistry*, 94, 5369-5380, doi: 10.1021/j100376a038, 1990.
- Clegg, S. L., Brimblecombe, P., and Wexler, A. S.: Thermodynamic model of the system  $\text{H}^+$ - $\text{NH}_4^+$ - $\text{SO}_4^{2-}$ - $\text{NO}_3^-$ - $\text{H}_2\text{O}$  at tropospheric temperatures, *J. Phys. Chem. A*, 102, 2137-2154, doi: 10.1021/Jp973042r, 1998.
- Fountoukis, C., and Nenes, A.: ISORROPIA II: a computationally efficient thermodynamic equilibrium model for  $\text{K}^+$ - $\text{Ca}^{2+}$ - $\text{Mg}^{2+}$ - $\text{NH}_4^+$ - $\text{Na}^+$ - $\text{SO}_4^{2-}$ - $\text{NO}_3^-$ - $\text{Cl}^-$ - $\text{H}_2\text{O}$  aerosols, *Atmos. Chem. Phys.*, 7, 4639-4659, doi: 10.5194/acp-7-4639-2007, 2007.
- Guo, H., Xu, L., Bougiatioti, A., Cerully, K. M., Capps, S. L., Hite, J. R., Carlton, A. G., Lee, S. H., Bergin, M. H., Ng, N. L., Nenes, A., and Weber, R. J.: Fine-particle water and pH in the southeastern United States, *Atmos. Chem. Phys.*, 15, 5211-5228, doi: 10.5194/acp-15-5211-2015, 2015.
- Guo, H., Sullivan, A. P., Campuzano-Jost, P., Schroder, J. C., Lopez-Hilfiker, F. D., Dibb, J. E., Jimenez, J. L., Thornton, J. A., Brown, S. S., Nenes, A., and Weber, R. J.: Fine particle pH and the partitioning of nitric acid during winter in the northeastern United States, *J. Geophys. Res.*, 121, 10355-10376, doi: 10.1002/2016jd025311, 2016.
- Guo, H., Liu, J., Froyd, K. D., Roberts, J. M., Veres, P. R., Hayes, P. L., Jimenez, J. L., Nenes, A., and Weber, R. J.: Fine particle pH and gas-particle phase partitioning of inorganic species in Pasadena, California, during the 2010 CalNex campaign, *Atmos. Chem. Phys.*, 17, 5703-5719, doi: 10.5194/acp-17-5703-2017, 2017a.
- Guo, H., Weber, R. J., and Nenes, A.: High levels of ammonia do not raise fine particle pH sufficiently to yield nitrogen oxide-dominated sulfate production, *Sci. Rep.*, 7, doi: 10.1038/s41598-017-11704-0, 2017b.
- Hennigan, C. J., Izumi, J., Sullivan, A. P., Weber, R. J., and Nenes, A.: A critical evaluation of proxy methods used to estimate the acidity of atmospheric particles, *Atmos. Chem. Phys.*, 15, 2775-2790, doi: 10.5194/acp-15-2775-2015, 2015.
- Liu, M., Song, Y., Zhou, T., Xu, Z., Yan, C., Zheng, M., Wu, Z., Hu, M., Wu, Y., and Zhu, T.: Fine particle pH during severe haze episodes in northern China, *Geophys. Res. Lett.*, 44, 5213-5221, doi: 10.1002/2017gl073210, 2017.
- Schlag, P., Kiendler-Scharr, A., Blom, M. J., Canonaco, F., Henzing, J. S., Moerman, M., Prévôt, A. S. H., and Holzinger, R.: Aerosol source apportionment from 1-year measurements at the CESAR tower in Cabauw, the Netherlands, *Atmos. Chem. Phys.*, 16, 8831-8847, doi: 10.5194/acp-16-8831-2016, 2016.
- Wang, G., Zhang, R., Gomez, M. E., Yang, L., Levy Zamora, M., Hu, M., Lin, Y., Peng, J., Guo, S., Meng, J., Li, J., Cheng, C., Hu, T., Ren, Y., Wang, Y., Gao, J., Cao, J., An, Z., Zhou, W., Li, G., Wang, J., Tian, P., Marrero-Ortiz, W., Secrest, J., Du, Z., Zheng, J., Shang, D., Zeng, L., Shao, M., Wang, W., Huang, Y., Wang, Y., Zhu, Y., Li, Y., Hu, J., Pan, B., Cai, L., Cheng, Y., Ji, Y., Zhang, F., Rosenfeld, D., Liss, P. S., Duce, R. A., Kolb, C. E., and Molina,

Formatted: Font:(Default) Calibri, 12 pt, Do not check spelling or grammar

- M. J.: Persistent sulfate formation from London Fog to Chinese haze, *Proc. Natl. Acad. Sci. U.S.A.*, 113, 13630-13635, doi: 10.1073/pnas.1616540113, 2016.
- Xu, L., Suresh, S., Guo, H., Weber, R. J., and Ng, N. L.: Aerosol characterization over the southeastern United States using high-resolution aerosol mass spectrometry: spatial and seasonal variation of aerosol composition and sources with a focus on organic nitrates, *Atmos. Chem. Phys.*, 15, 7307-7336, doi: 10.5194/acp-15-7307-2015, 2015.